Multiple porphyry Cu-Mo events in the Eastern Pontides metallogenic belt, Turkey: From Early Cretaceous subduction to Eocene post-collision evolution

Okan Delibaş[1†], Robert Moritz[2]*, David Selby[3],

Deniz Göç[4], Mustafa Kemal Revan[4]

[1]: *Hacettepe University, Department of Geological Engineering, 06800, Beytepe-Ankara, Turkey*

[2]:*Department of Earth Sciences, University of Geneva, Rue des Maraîchers 13, 1205 Geneva, Switzerland*

[3]:*Durham University, Department of Earth Sciences, Durham DH1 3LE, United Kingdom*

[4]: *General Directorate of Mineral Research and Exploration (MTA), 06800, Ankara, Turkey*

†Deceased: August 24th, 2016

*Corresponding author. Postal address: University of Geneva, Department of Earth Sciences, Rue des Maraîchers 13, 1205 Geneva, Switzerland. Phone: +41223796633, e-mail: robert.moritz@unige.ch

Abstract

Four porphyry Cu-Mo systems were investigated by Re-Os molybdenite geochronology to constrain their timing with respect to the geodynamic and magmatic evolution of the Eastern Pontides, Turkey. Molybdenite from the Ispir-Ulutaş deposit yielded a Re-Os age of 131.0±0.7 Ma, which is consistent with Early Cretaceous U-Pb LA-ICP-MS zircon ages of local calc-alkaline intrusions. It demonstrates that porphyry deposits were already formed during Early Cretaceous subduction of the Neotethys along the Eastern Pontides, and that they can be correlated with porphyry Cu events in the adjacent Lesser Caucasus. Molybdenite Re-Os ages of 76.0±0.4 and 75.7±0.4 Ma at the Elbeyli prospect and 77.2±1.0 Ma at the Emeksen prospect overlap with U-Pb LA-ICP-MS zircon ages of shoshonitic to high-K calc-alkaline intrusions in the region, which were emplaced during Late Cretaceous Neotethys subduction. A 50.7±0.3 Ma molybdenite Re-Os age at the Güzelyayla deposit confirms porphyry Cu-Mo emplacement coeval with Eocene post-collisional, calc-alkaline adakitic magmatism of the Eastern Pontides.

An electron microprobe study of molybdenite samples, supplemented by data obtained during Re-Os dating, shows that the Eocene Güzelyayla deposit and the Late Cretaceous Emeksen prospect have the highest Re-enrichment. Post-collisional melting of a thickened mafic lower continental crust and melting of a metasomatized lithospheric mantle with little to no interaction with upper crustal rocks may explain the Re enrichment at Güzelyayla and Emeksen, respectively.

Introduction

The Turkish Eastern Pontides record Mesozoic to Cenozoic subduction of the Neotethys along the Eurasian margin, followed by collision with Gondwana-derived terranes (Adamia et al., 1981, 2011; Şengör and Yilmaz, 1981; Kazmin et al., 1986; Okay and Şahintürk, 1997; Okay,

2008; Dokuz et al., 2010; Karsli et al., 2011, 2012; Kaygusuz and Şen, 2011). They host mainly volcanogenic massive sulfide (VMS), porphyry and epithermal deposits and prospects, and subsidiary skarn and carbonate-hosted base metal prospects (Fig. 1; Yigit, 2009).

Ore deposit studies and exploration efforts in the Eastern Pontides were mostly focused on VMS deposits (e.g. Çağatay and Boyle, 1977; Pejatoviç, 1979; Akıncı, 1980, 1984; Çağatay, 1993; Karakaya et al., 2012; Eyuboglu et al., 2014; Revan et al., 2014, 2017b). By contrast, knowledge about porphyry-epithermal systems, which are typically interpreted as Late Cretaceous to Eocene in this metallogenic belt (Soylu, 1999; Yigit, 2009), remains fragmentary (Delibaş et al., 2016 and references therein). Thus, in this contribution, we focus our study on four porphyry prospects and deposits of the Eastern Pontides, which were investigated by the General Directorate of Mineral Research and Exploration of Turkey (MTA, 1984, 2002), because of their molybdenite-rich nature. They include the Elbeyli and Emeksen prospects, and the Güzelyayla and Ispir-Ulutaş deposits (Fig. 1), the characteristics of which are summarized in the first part of this contribution. Molybdenite samples were collected at the four study areas and were dated by Re-Os geochronology. These new age data together with published intrusion U-Pb zircon ages allow us to discuss the timing of porphyry mineralization within the geodynamic and magmatic evolution of the Eastern Pontides. Finally, since porphyry deposits are the major source of Re (Millensifer et al., 2014), we have conducted a preliminary study of the Re content of molybdenite, which mainly hosts this element in porphyry deposits (Berzina et al., 2005; Sinclair and Jonasson, 2014). This allows us to discuss the Re potential in porphyry systems of the Eastern Pontides.

Geodynamic and Regional Setting

The Eastern Pontides and its eastern extension in the Lesser Caucasus represent the southern active margin of Eurasia during northward to northeastward subduction of the Neotethys since the Middle Jurassic (Adamia et al., 1981, 2011; Şengör and Yilmaz, 1981; Okay and Şahintürk, 1997; Rolland et al., 2011; Topuz et al., 2013). Neotethys subduction was followed by amalgamation with the Gondwana-derived Anatolide-Tauride block from Late Cretaceous to Eocene (Şengör and Yilmaz, 1981; Okay and Şahintürk, 1997; Yilmaz and Tüysüz, 1997; Okay and Tüysüz, 1999; Topuz et al., 2011; Okay and Nikishin, 2015).

The Variscan basement of the Eastern Pontides is principally made up of Carboniferous metamorphic, sedimentary, gabbroic, and granitic rocks, and Permo-Triassic oceanic rocks (Şengör et al., 1980; Okay and Şahintürk, 1997; Topuz et al., 2004a,b, 2007, 2010; Ustaömer and Robertson, 2010; Ustaömer et al., 2012; Okay and Nikishin, 2015; Okay and Topuz, 2017). The basement units are unconformably overlain by Early to Middle Jurassic volcanoclastic rocks and Late Jurassic to Early Cretaceous platform carbonate rocks (Şen, 2007; Kandemir and Yilmaz, 2009; Dokuz et al., 2010; Ustaömer and Robertson, 2010). Jurassic magmatic rocks intruding into the Permo-Triassic rocks are attributed to a back-arc setting during northward subduction of the Tethys (Ustaömer et al., 2012; Topuz et al., 2013).

According to Okay and Şahintürk (1997), the Eastern Pontides volcanic arc developed predominantly during the Turonian to Maastrichtian. However, calc-alkaline plutonic rocks were already emplaced during the Early Cretaceous in the eastern part of the tectonic province (Giles, 1973; Boztuğ et al., 2006; Boztuğ and Harlavan, 2008; Chen et al., 2016; Delibaş et al., 2016). Arc-related tholeiitic, calc-alkaline to shoshonitic Late Cretaceous magmatism, including abundant granitic to monzodioritic intrusions, is attributed to subduction of the northern branch

of the Neotethys (Peccerillo and Taylor, 1975; Eğin et al., 1979; Manetti et al., 1983; Boztuğ and Harlavan, 2008; Karsli et al., 2010, 2012; Kaygusuz et al., 2013, 2014; Delibaş et al., 2016).

The collision between the Eastern Pontides and the Anatolide-Tauride block during the Late Cretaceous to early Cenozoic resulted in crustal shortening, thickening and uplift (Okay and Şahintürk, 1997; Yilmaz and Tüysüz, 1997; Okay and Tüysüz, 1999; Okay and Nikishin, 2015). Post-collision magmatism includes early Eocene adakitic and middle Eocene to middle Miocene-Pliocene alkaline, calc-alkaline, and tholeiitic rocks (Arslan and Aslan, 2006; Aydın et al., 2008; Boztuğ and Harlavan, 2008; Okay, 2008; Topuz et al., 2011; Temizel et al., 2012).

Investigated Porphyry Prospects and Deposits

Elbeyli porphyry prospect

The Elbeyli prospect is located within the westernmost part of the Eastern Pontides (Fig. 1). Recent drilling has documented an approximately 200 m-deep zone below surface with local, discrete zones enriched in gold with contents up to 1 ppm. The Elbeyli prospect is spatially associated with a Late Cretaceous shoshonitic monzonite/monzodiorite dated at 77.0±1.3 Ma, which intruded a Cretaceous arc-related volcanic and volcano-sedimentary sequence, including andesitic and dacitic lava and pyroclastic rocks intercalated with marl, mudstone and siltstone units (Delibaş et al., 2016; Fig. 2).

The prospect consists of a quartz-pyrite-chalcopyrite stockwork (Fig. 3a), east- and NE-trending quartz-pyrite veins, and late NW-trending quartz-molybdenite and quartz-pyrite-enargite-chalcopyrite-tennantite-molybdenite veins (Fig. 2: location i29-y, quartz-molybdenite vein zone; Fig. 3b-c) hosted by Late Cretaceous andesite-dacite and monzonite/monzodiorite. In the later veins, the high-sulfidation state sulfide mineral assemblage consists of enargite, euhedral pyrite and covellite, and is followed by an intermediate-sulfidation state mineral assemblage

including chalcopyrite and tennantite, accompanied by molybdenite and rutile. Euhedral pyrite and enargite are partly replaced by tennantite along rims and cracks (Fig. 3g). Molybdenite precipitated along fractures in pyrite (Fig. 3h). Minor native bismuth is also present, and 1 to 5 mm-thick galena veins crosscut the former ore minerals. No visible gold was identified during reflected light microscopy, despite the drilling results mentioned above.

The immediate host rocks of the veins were affected by pervasive sericitic-chloritic and transitional sericitic to advanced argillic alteration, which resulted locally in intensively silicified zones with disseminated molybdenite (Fig. 3d). The sericitic-chloritic alteration assemblage consists of fine-grained muscovite, chlorite and epidote. A remnant potassic alteration assemblage consists of rare ~0.5-1cm-thick K-feldspar and magnetite veins in the eastern part of the prospect (Fig. 2). A propylitic alteration assemblage at the periphery of the mineralized rocks consists of a chlorite-epidote-calcite assemblage with a pyrite-rich stockwork (Fig. 2).

The transitional sericitic to advanced argillic alteration assemblage and the silicified rock are more intensively developed with increasing density of the fracture and fault network. The transitional sericitic to advanced argillic alteration assemblage is composed of pyrophyllite, quartz, and zunyite (Fig. 3e-f), which are accompanied by aluminium-phosphate-sulfate minerals, fluorite, kaolinite and minor sericite. Local, pyrophyllite pseudomorphs after andalusite can be recognized. This alteration zone shares many features with the roots of advanced argillic alteration zones described in porphyry systems (Sillitoe, 2010; Voudouris and Melfos, 2012).

Emeksen porphyry prospect

The Emeksen porphyry prospect is situated about 40 km SE of the Elbeyli prospect (Fig. 1). An exploration program of the MTA (1984) reported Mo grades between 0.08 and 2.87 wt% for veins from this prospect. Neither gold nor copper contents have been reported by the MTA

(1984) study and in a PhD study by Doğan (1980). Kamitani et al. (1977) describe Pb-Zn veins hosted by Cretaceous volcanic rocks along the eastern parts of the intrusive rocks of the prospect (outside of the map area, not shown in Figure 4), with Ag and Au contents up to 78 ppm and 8 ppm, respectively. Early Mesozoic metamorphic rocks are unconformably overlain by Cretaceous volcanic and volcano-sedimentary rocks (Kamitani et al., 1977). The ore zones are hosted by calc-alkaline to high-K calc-alkaline granodiorite, granite and porphyritic granite with gradational contacts between each other, intruding the Cretaceous volcanic and volcano-sedimentary rocks (Fig. 4). The granodiorite, granite and porphyritic granite have yielded U-Pb LA-ICP-MS zircon ages of 78.7±0.5 Ma, 78.5±0.5 Ma and 77.7±0.5 Ma, respectively (Delibaş et al., 2016).

The porphyry system at the Emeksen prospect consists of isolated veins and stockwork. Veins are subdivided into NW-striking quartz-molybdenite and north-striking quartz-molybdenite-pyrite veins (Fig. 5a-b; Kamitani et al., 1977; Doğan, 1980). Some of the quartz-molybdenite-pyrite veins are banded, with pyrite- and molybdenite-rich ~2-3 cm-thick bands alternating with quartz bands (Fig. 5d). An additional ore type consists of disseminated molybdenite and pyrite within the silicified zones of the Emeksen granite (Fig. 5c). Arsenopyrite, minor amounts of native gold as well as electrum are associated with the quartz veins (Fig. 5e). Fahlore minerals and rutile are also present.

The hydrothermal alteration assemblages at the prospect are confined to the immediate vein zones (Doğan, 1980). The alteration assemblage along the veins is characterized by muscovite and minor chlorite replacement, respectively, of feldspar and biotite (Fig. 5a-b). The sericitic-chloritic alteration halo passes outwards to an epidote-, chlorite- and calcite-bearing alteration assemblage, replacing partly to totally biotite and feldspar. Potassic alteration locally affected the granodiorite and the porphyry granite, characterized by biotite clusters and veins (Fig. 5f).

Güzelyayla porphyry deposit

The Güzelyayla Cu-Mo deposit lies within the central part of the Eastern Pontides metallogenic belt, about 20 km SW of the Trabzon town (Fig. 1). Güzelyayla is the first porphyry deposit with significant Cu and Mo resources that has been discovered in the Eastern Pontides (Nebioğlu, 1983; Güner and Güç, 1990; Soylu, 1999). Exploration results report 186.2 Mt of ore at 0.3 wt% Cu equivalent and 0.014 wt% Mo of total proven and probable reserves (JICA, 1987; Güner and Güç, 1990; Er et al., 1992). According to drill-hole data, a 10 to 30 m-thick supergene enrichment zone contains 0.8 wt% Cu equivalent (Çınar and Yazıcı, 1985; Güner and Güç 1990). The geology of the Güzelyayla area consists of Late Cretaceous andesitic lava and pyroclastic rocks, with siltstone, mudstone and limestone intercalations (Nebioğlu, 1983; Çınar and Yazıcı 1985), which have been intruded by Late Cretaceous porphyritic granite and dacite (Aydın, 2014; Fig. 6). The latter was dated at 81.4±1.1 Ma by U-Pb LA-ICP-MS zircon geochronology (Delibaş et al., 2016). The youngest magmatic event consists of late Eocene sub-volcanic granodioritic to tonalitic porphyritic dikes, which yielded $^{40}Ar/^{39}Ar$ hornblende ages of 53.55±0.34 and 51.34±0.27 Ma (Karsli et al., 2011).

Mineralization types at the Güzelyayla deposit consists of early stockwork veins (Fig. 7a-b), late stage NW-oriented 0.1 to 4 cm-thick quartz veins (Fig. 7c), and disseminated opaque mineral assemblages (Çınar and Yazıcı, 1985). Molybdenite is mainly enriched in the late stage quartz veins crosscutting the Late Cretaceous porphyritic dacitic intrusion and its immediate country rocks (Fig. 7c). Stockwork-type quartz veins contain chalcopyrite, pyrite, pyrrhotite, rutile and minor molybdenite (Fig. 7e). Late stage NW-oriented quartz veins contain pyrite, chalcopyrite, molybdenite and sericite. Disseminated opaque mineral assemblages consist of chalcopyrite, bornite, magnetite, pyrite, and minor molybdenite. Covellite, chalcocite and digenite are interpreted as secondary minerals, related to local supergene enrichment (Fig. 7f).

Drill-holes have crosscut a skarn zone between the porphyritic dacitic intrusion and limestone, which contain magnetite and minor chalcopyrite, pyrite and malachite (Güner and Güç, 1990).

The central part of the porphyritic dacite was affected by potassic alteration (Fig. 6) with partial to complete replacement of amphibole by biotite and the presence of biotite veins and clusters, and disseminated magnetite. The potassic zone is crosscut by thin quartz and sericite veins (Fig. 7d) and secondary biotite is replaced by chlorite. A sericitic alteration assemblage overprints the porphyritic dacitic intrusion, and the volcanic and volcano-sedimentary country rocks. It is characterized by sericite and pyrite veins associated with the molybdenite-bearing veins. A distal propylitic alteration assemblage is developed in the volcanic and volcanoclastic country rocks and is crosscut by a stockwork consisting of pyrite veins and overprinted by iron oxides (Çınar and Yazıcı, 1985; Güner and Güç, 1990; Soylu, 1999).

Ispir-Ulutaş porphyry deposit

The Ispir-Ulutaş porphyry-type Cu-Mo deposit is located in the southeastern part of the Eastern Pontides (Fig. 1), and contains 73.6 Mt ore reserves at a grade of 0.35 wt% Cu and 0.03 wt% Mo (Giles, 1973; Soylu, 1999; Yiğit, 2009; http://www.demirexport.com). A subsidiary skarn zone contains 3 Mt ore reserves at 1.3 wt% Cu, 4.77 wt% Zn and 33 ppm Ag (http://www.demirexport.com). The basement is composed of Paleozoic to Early Mesozoic metamorphic rocks, and is overlain by weakly metamorphosed and folded Cretaceous dacitic to rhyolitic lava flows intercalated with mudstone, shale and conglomerate (Fig. 8; Giles, 1973; Taylor and Fryer, 1980). These rock units are crosscut by the composite calc-alkaline Early Cretaceous Ispir batholith dated by K-Ar geochronology at 132±5 Ma (Giles, 1973). The Ispir batholith consists predominantly of porphyritic granodiorite and porphyritic rhyolite to latite with quartz phenocrysts, which were dated at 132.9±0.6 and 131.1±0.9 Ma, respectively, by U-Pb LA-

ICP-MS zircon geochronology (Delibaş et al., 2016). Subsidiary magmatic rocks are gabbroic-dioritic intrusions. Late Paleocene to middle Eocene calc-alkaline basaltic to andesitic lava flows, tuff and agglomerate overlay the older rock units, followed by Pleistocene to recent glacial debris (Fig. 8; Giles, 1973; Taylor and Fryer, 1980).

The Ispir-Ulutaş deposit consists of porphyry-type Cu-Mo ore bodies (Taylor and Fryer, 1980; Soylu 1999), accompanied by a Cu-Zn skarn in the metamorphic basement units (http://www.demirexport.com; Fig. 8). The porphyry Cu-Mo is centered on the calc-alkaline porphyritic granite and the porphyritic rhyolitic to latitic intrusions. It consists of stockwork-type ore zones and isolated NW-oriented quartz veins (Fig. 9a-b). The stockwork-type quartz veins contain pyrite, chalcopyrite, molybdenite, sphalerite, and hematite (Fig. 9c), as well as pyrrhotite inclusions within pyrite. The NW-oriented veins contain predominantly pyrite with minor molybdenite and chalcopyrite fractures in pyrite. Covellite replaces chalcopyrite along its rims. Rutile and hematite are present within the immediate host rocks of the NW-striking veins.

Sericitic and argillic alteration have affected the Cretaceous rocks of the porphyry Cu-Mo deposit (Fig. 8). The sericitic alteration assemblage consists of muscovite, sericite, pyrite (Fig. 9d) and calcite, accompanied by small quartz and calcite veins. The argillic alteration assemblage consists of kaolinite and intensively silicified rocks. The intensity of the sericitic alteration assemblage is directly correlated with the density of the mineralized vein network (Taylor and Fryer, 1980). Taylor and Fryer (1980) report a potassic alteration assemblage in the porphyritic rhyolitic to latitic intrusions and the porphyritic granodiorite consisting of hydrothermal biotite and K-feldspar together with quartz (Fig. 8). A distal propylitic alteration halo is recognized in the metamorphic basement (Fig. 8), the Cretaceous volcanic and sedimentary sequence, and the porphyritic rhyolitic to latitic intrusions. It consists in chlorite, epidote, calcite, and locally albite, hematite and pyrite. According to Taylor and Fryer (1980), the propylitic alteration assemblage is

accompanied by pyrite-sphalerite-galena and barite-calcite veins, and it overprints a potassic mineral assemblage in marginal areas of the composite magmatic intrusion.

Analytical Techniques

For Re-Os dating, the molybdenite samples were ground and sieved to collect the 63 to 315 μm fraction. Molybdenite was concentrated by heavy liquids and purified by flotation using deionized water in an ultrasonic bath. All samples were hand picked under a binocular magnifier to remove remaining impurities. The ^{187}Re and ^{187}Os concentrations in molybdenite were determined by isotope dilution negative thermal ionization mass spectrometry at the University of Durham, United Kingdom. Detailed analytical procedures are described by Selby and Creaser (2001). In brief, analyses were conducted on a Thermo TRITON mass spectrometer, with the Re and Os isotopic compositions measured using static Faraday collection. The Carius tube method was used for the dissolution of molybdenite and equilibration of sample and tracers of Re and Os. Total procedural blanks for Re and Os were 2 pg and 0.5 pg, respectively, with an ^{187}Os/^{188}Os blank ratio of 0.24 ± 0.02 (n = 6). Rhenium and Os concentrations and Re-Os molybdenite date uncertainties are presented at the 2σ level (Table 1), which includes the uncertainties in Re and Os mass spectrometer measurement, spike and standard Re and Os isotopic compositions, and calibration uncertainties of ^{185}Re and ^{187}Os. All data are blank corrected, even though blank levels are insignificant to the quantities of Re and Os measured in the molybdenite samples.

Molybdenite mineral compositions were determined using a Cameca SX50 wavelength-dispersive electron microprobe (EMPA) at the University of Lausanne, Switzerland. The analyzed molybdenites were pure minerals. Scanning electron microscopy and microprobe images did not detect the presence of any other Re-bearing mineral phase in the analyzed molybdenite. Operating conditions were 20kv for the accelerating voltage and 30nA for the beam

current with a 10μm probe diameter. Pyrite (for S and Fe), bornite (for Cu), molybdenite (for Mo), and Re-metal (for Re) standards were used. Detection limit was 0.8wt% for Re.

Results

Molybdenite Re-Os geochronology

Five molybdenite samples were dated. Two molybdenite samples from the Elbeyli prospect were collected from two different outcrops (Fig. 2): sample OEY-1 is from a NW-oriented quartz-molybdenite vein from the transitional zone between the advanced argillic and sericite-chlorite alteration zones (Fig. 3c), and sample i29-y was taken from a molybdenite-quartz-rutile-pyrite-rich area in the advanced argillic zone (Fig. 3d and h). The Elbeyli samples OEY-1 and i29-y yielded Re-Os ages of 76.0±0.4 Ma and 75.7±0.4 Ma, respectively (Table 1). At the Emeksen prospect (Fig. 4), the EGY-1 sample was collected from a NW-oriented quartz-molybdenite-pyrite vein crosscutting highly sericitized granite (Fig. 5a). It yielded a Re-Os age of 77.2±1.0 Ma (Table 1). At the Güzelyayla deposit (Fig. 6), sample H-1 was taken from a stockwork-type vein system crosscutting the sericitized porphyritic dacite (Fig. 7b), and yielded a Re-Os age of 50.7±0.3 Ma (Table 1). At the Ispir-Ulutaş deposit (Fig. 8), sample U-2 was collected from a pyrite-molybdenite-chalcopyrite-bearing stockwork hosted by sericitized porphyritic rhyolite to latite (Fig. 9a), and yielded a Re-Os age of 131.0±0.7 Ma (Table 1).

Re contents of molybdenite samples

Molybdenite Re contents were obtained during Re-Os age determinations (Table 1), and by EMPA with a total of 61 different spots analyzed on molybdenite samples from the four different study areas (Table 2). Rhenium contents are below detection limits by EMPA (<0.8

wt% Re) in the Emeksen and Ispir-Ulutaş samples (Table 2), which are consistent with low Re contents between 9.7 and 150 ppm yielded by mass spectrometry during Re-Os geochronology (Table 1). By contrast, several Elbeyli and Güzelyayla molybdenite samples yielded high Re contents between 820 and 3409 ppm (Table 2), consistent with elevated Re concentrations of 368 to 6992 ppm obtained during Re-Os geochronology (Table 1). The Re concentrations of molybdenite samples from the Güzelyayla deposit broadly increase with decreasing Mo concentrations. On the other hand, the Elbeyli molybdenite samples display two trends: Mo contents are variable and uncorrelated with Re concentrations below 1800 ppm, whereas Mo contents remain constant at 60.6-60.8 wt% for Re concentrations in excess of 1800 ppm (Fig. 10).

Our study at Güzelyayla documents a Re-enrichment over time between the two molybdenite generations distinguished in this deposit (Fig. 10). Indeed, out of 14 EMPA analyses of molybdenite collected from the early stage stockwork (sample H1 in Table 2), 10 EMPA spot analyses were below detection limit (<0.8 wt% Re), which is consistent with the low Re content of 368 ppm obtained during Re-Os age determination (Table 1), and only 4 EMPA spot analyses yielded Re contents exceeding the detection limit (>0.8 wt% Re), that is between 1030 and 1469 ppm (Table 2; Fig. 10). By contrast, one molybdenite sample from an isolated, late stage quartz vein crosscutting the porphyritic dacite is enriched in Re, with nearly all EMPA spot analyses yielding Re concentrations above the detection limit (>0.8 wt% Re) and up to 3409 ppm (sample TMM1 in Table 2; Fig. 10).

Discussion

Timing of porphyry events in the Eastern Pontides and regional correlations

Porphyry systems in the Eastern Pontides are typically interpreted as Late Cretaceous to Eocene (Soylu, 1999; Yigit, 2009). Our study demonstrates that porphyry ore formation in the Eastern Pontides is older than previously recognized, and certainly opens up new exploration avenues. Our new Re-Os molybdenite ages indicate multiple porphyry mineralization events in the Eastern Pontides from the Early Cretaceous to the early Eocene (Fig. 11).

The 131.0±0.7 Ma Re-Os age for molybdenite from the Ispir-Ulutaş deposit (Table 1) coincides with the Early Cretaceous magmatic events in the same location dated by U-Pb LA-ICP-MS and K-Ar ages (Fig. 11). In particular, the Re-Os molybdenite age overlaps within uncertainty with the U-Pb LA-ICP-MS zircon age of 131.1±0.9 Ma of the porphyritic rhyolitic to latitic intrusion (Delibaş et al., 2016; Fig. 11). Thus, porphyry Cu-Mo mineralization at Ispir-Ulutaş coincided with regional Early Cretaceous calc-alkaline magmatism during Neotethys subduction along the Eastern Pontides (Giles, 1973; Yilmaz et al., 2000, 2004; Boztuğ et al., 2006; Boztuğ and Harlavan, 2008; Ustaömer and Robertson, 2010; Chen et al., 2016; Delibaş et al., 2016). The 131.0±0.7 Ma Re-Os molybdenite age from the Ispir-Ulutaş deposit indicates that the Early Cretaceous porphyry Cu-Mo event in the Eastern Pontides belongs to a regional metallogenic event along the Eurasian margin. Indeed, it can be traced eastwards into the calc-alkaline Somkheto-Karabagh magmatic belt of the Lesser Caucasus, where the Teghout porphyry deposit, Armenia was formed at 145.85±0.59 Ma and the Kharkhar porphyry prospect in Azerbaijan at 133.27±0.53 Ma (Fig. 11; Moritz et al., 2016).

The Re-Os molybdenite ages at the Emeksen and Elbeyli prospects confirm the regional Late Cretaceous porphyry event in the Eastern Pontides as reported in earlier studies (e.g., Yigit, 2009). At the Emeksen prospect, the Re-Os molybdenite age of 77.2±1.0 Ma (Table 1) overlaps

within uncertainty with the U-Pb LA-ICP-MS zircon age of the associated 77.7±0.5 Ma porphyritic granite (Fig. 11; Delibaş et al. 2016). Molybdenite samples from the Elbeyli prospect have yielded Re-Os ages of 76.0±0.4 and 75.7±0.4 Ma (Table 1), which overlap within analytical uncertainty with the 77.0±1.3 Ma U-Pb LA-ICP-MS zircon age of the host porphyritic granite (Fig. 11; Delibaş et al., 2016). The U-Pb and Re-Os ages indicate that the Late Cretaceous porphyry event coincides with final subduction evolution of the northern branch of the Neotethys, before Late Cretaceous-early Cenozoic collision between the Eastern Pontides and the Anatolide-Tauride block (Okay and Şahintürk, 1997; Yilmaz and Tüysüz, 1997; Okay and Tüysüz, 1999; Topuz et al., 2011; Okay and Nikishin, 2015). Furthermore, the Late Cretaceous porphyry event postdates the magmatic rocks hosting volcanogenic massive sulfide ore, which yielded U-Pb ages between 91.1±1.3 Ma and 82.6±0.8 Ma (Eyuboglu et al., 2014; Revan et al., 2017b; Fig. 11).

The Re-Os molybdenite age of 50.7±0.3 Ma at Güzelyayla demonstrates that the porphyry event postdates the Late Cretaceous porphyritic dacite host, which yielded a U-Pb LA-ICP-MS zircon age of 81.4±1.1 Ma (Fig. 11; Delibaş et al., 2016). It documents a distinctly younger mineralization event at the end or shortly after intrusion of Eocene adakitic granodioritic and tonalitic porphyritic dikes crosscutting the Late Cretaceous volcano-sedimentary sequence, which have yielded 53.55±0.34 and 51.34±0.27 Ma $^{40}Ar/^{39}Ar$ hornblende ages (Fig. 6; Karsli et al., 2011). Thus the Güzelyayla porphyry event is closely linked to adakitic magmatism attributed to partial melting of a thickened lower crust during post-collisional evolution of the Eastern Pontides (Yilmaz and Boztuğ, 1996; Topuz et al., 2005, 2011). This post-collisional metallogenic evolution (Fig. 11) also includes the Bakircay prospect dated at 38.6±1.3 and 37.4±1.3 Ma by K-Ar on biotite (Taylor, 1981), epithermal mineralization at ~47-48 Ma dated by U-Pb geochronology (Bilir, 2015), the Balcili porphyry Cu-Mo prospect, which yielded a K-Ar age of 62.3±4.2 Ma (Soylu, 1999), and a porphyry system at Ulutas dated at 59 Ma (Yigit; 2009).

Rhenium potential of porphyry systems from the Eastern Pontides and genetic implications

Our investigation allows us to define some broad controls explaining the variable Re-enrichments in porphyry systems from the Eastern Pontides. Molybdenite samples from the Elbeyli prospect and the Güzelyayla deposit yielded the highest Re concentrations (Table 2; Fig. 10). The large variation of Re contents yielded by EMPA spot analyses of single molybdenite crystals of this investigation is consistent with other studies documenting heterogeneity of Re distribution at the grain-scale (e.g., Rathkopf et al., 2017). Such grain-scale heterogeneity cannot be identified by mass spectrometry determination of Re contents, which is based on the dissolution of bulk molybdenite samples and yields only averaged mineral compositions. The elevated Re concentrations in molybdenite samples from Elbeyli and Güzelyayla are consistent with other studies reporting Re contents of several thousand of ppm in molybdenite from porphyry environments (e.g. Berzina et al., 2005; Voudouris et al., 2009, 2013; Rathkopf et al., 2017), as well as with experimental studies demonstrating that molybdenite can incorporate up to 2.7 and 2.2 wt% Re, respectively, at 1000 and 400°C (Drábek et al., 2010).

At the Güzelyayla Cu-Mo deposit, the early Eocene sub-volcanic adakitic dikes coeval with ore formation were generated during post-collisional magmatism linked to melting of a thickened mafic lower continental crust (Karsli et al., 2011; Chen et al., 2016). This geodynamic setting combined with Re-enrichment in the early Cenozoic porphyry deposit from the Eastern Pontides is reminiscent of the Cenozoic setting in the northern Aegean region in Greece, where molybdenite samples from post-subduction porphyry-epithermal systems are considerably enriched in Re. Rhenium-enrichment in the northern Aegean region is attributed to magmas sourced from a strongly metasomatized mantle source and produced by melting of lower crustal amphibolitic cumulate rocks (Voudouris et al., 2013). The latter source is consistent with the

interpretation for the Eocene adakitic magmatism in the Eastern Pontides (Karsli et al., 2011), and may explain the Re-enriched nature of molybdenite from the Güzelyayla deposit.

The Elbeyli and Emeksen porphyry prospects are coeval Late Cretaceous systems and belong to the same subduction setting (Fig. 11). However, only molybdenite from the Elbeyli prospect yielded high Re concentrations (Table 2; Fig. 10). The contrasting Re-content of molybdenite from both prospects can be explained by different petrogenetic evolutions of the associated Late Cretaceous intrusive rocks. At Elbeyli, the primitive Sr and Nd isotopic compositions ($^{87}Sr/^{86}Sr_{initial}$ = 0.70478 to 0.70482 and $^{143}Nd/^{144}Nd_{initial}$ = 0.512574 to 0.512602; Delibaş et al., 2016) of the shoshonitic monzonite/monzodiorite coeval with ore formation are consistent with melts derived from a mantle source, which had little to no interaction with upper crustal rocks. By contrast, at the Emeksen prospect, the granodiorite, granite and porphyritic granite contemporaneous with ore formation document a higher degree of magmatic fractionation, and their Sr and Nd isotopic compositions ($^{87}Sr/^{86}Sr_{initial}$ = 0.70567 to 0.70780 and $^{143}Nd/^{144}Nd_{initial}$ = 0.512296 to 0.512435; Delibaş et al., 2016) indicate significant interaction of the magmas with upper crustal rocks (Delibaş et al., 2016). In brief, the Re-enrichment at Elbeyli is consistent with the consensus that mantle-derived magmas, which had negligible to no crustal interaction and experienced only moderate magmatic fractionation, are favorable settings for generating Re-enriched porphyry systems (Stein et al., 2001; Berzina et al., 2005; Voudouris et al., 2013; Sinclair and Jonasson, 2014; Zhong et al., 2016; Chen et al., 2017).

Conclusions

The four study areas of this contribution document episodic porphyry ore formation during the Mesozoic to Cenozoic geodynamic evolution of the Eastern Pontides. Our study at the Ispir-Ulutaş deposit demonstrates that porphyry Cu-Mo systems were already emplaced during

the Early Cretaceous in the Eastern Pontides. They can be correlated with Early Cretaceous porphyry Cu deposits emplaced along the Somkheto-Karabagh belt in the Lesser Caucasus. This opens up new exploration avenues, since Early Cretaceous magmatic centers should also be considered as attractive targets in addition to Late Cretaceous and Paleogene magmatic systems.

The mineralization ages at Elbeyli and Emeksen support the conclusions of previous studies, and demonstrate porphyry ore formation during Late Cretaceous shoshonitic to high-K calc-alkaline magmatism. This metallogenic evolution coincides with final subduction evolution of the northern branch of the Neotethys, immediately before collision of the Anatolide-Tauride block and the Eurasian margin, i.e. the Eastern Pontides. The early Eocene age at Güzelyayla underscores the porphyry Cu-Mo potential of the post-collisional geological environment of the Eastern Pontides. Our study supports porphyry Cu-Mo ore formation associated with adakitic magmatism produced by melting of a thickened continental crust.

Analysis of molybdenite samples has documented variable Re-enrichments in the four study areas. Favorable geodynamic and magmatic settings for Re-enriched porphyry Cu-Mo systems in the Eastern Pontides were identified at the Güzelyayla deposit and the Elbeyli prospect. They include, respectively: (1) early Eocene adakitic post-collisional magmatism, and (2) Late Cretaceous, subduction-related shoshonitic (monzonitic/monzodioritic) magmatism produced by melting of a metasomatized lithospheric mantle, with limited to no interaction of the mantle melts with the upper crust.

Acknowledgements

The research was supported by the Hacettepe University Scientific Research Coordination Unit grants FHD-2015-7509 and FDS-2015-7004, and the Swiss National Science Foundation through research grants 200020-155928 and 200020-168996. This research was also partially supported

by the General Directorate of Mineral Research and Exploration, Turkey (MTA) by the Eastern Pontides Metallic Mineral Exploration Project-2014-32-13-08. During 2013-2014, Okan Delibaş was supported by a post-doctoral TUBITAK Scholarship (2219-International Post-Doctoral Research Fellowship Program) at the University of Geneva. David Selby acknowledges the TOTAL endowment fund. Seçil Delibaş and Burcu Kahraman (Hacettepe University) are thanked for providing various pieces of information allowing us to finalize the manuscript. The authors thank Hervé Rezeau (University of Geneva*)* for help during electron microprobe analyses, and Oktay Parlak and Mustafa Özkan (MTA) during field studies. We are also grateful to the support provided by Demir Export Company, especially Özcan Dumanlılar. Editorial comments and critical reviews by Dick Tosdal and Tim Baker allowed us to significantly improve the quality of the manuscript. This paper is dedicated to the memory of the senior author Okan Delibaş, who dramatically passed away in August 2016, while working on this manuscript. Okan still had so many plans for future scientific projects, his death is a big loss to all of us.

References

Adamia, S.A., Chkoutua, T., Kekelia, M., Lordkipanidze, M., Shavishvili, I., and Zakariadze, G., 1981, Tectonics of the Caucasus and adjoining regions: Implications for the evolution of the Tethys ocean: Journal of Structural Geology, v. 3, p. 437-447.

Adamia, S., Zakariadze, G., Chkhotua, T., Sadradze, N., Tsereteli, N., Chabukiani, A., and Gventsadze, A., 2011, Geology of the Caucasus: A review: Turkish Journal of Earth Sciences, v. 20, p. 489-544.

Akıncı, Ö.T., 1980, Major copper metallogenic units and genetic igneous complexes of Turkey: In Jankovic, S., and Sillitoe, R.H. (eds.), European Copper Deposits, Belgrade University Faculty Geology Mining, Belgrade, p. 208-219.

Akıncı, Ö.T., 1984, The Eastern Pontide volcano-sedimentary belt and associated massive sulphide deposits: Geological Society of London Special Publication 17, p. 415-428.

Arslan, M., and Aslan, Z., 2006, Mineralogy, petrography and whole-rock geochemistry of the Tertiary granitic intrusions in the Eastern Pontides, Turkey: Journal of Asian Earth Sciences, v. 27, p. 177-193.

Aydın, F., 2014, Geochronology, geochemistry, and petrogenesis of the Maçka subvolcanic intrusions: implications for the Late Cretaceous magmatic and geodynamic evolution of the eastern part of the Sakarya Zone, northeastern Turkey: International Geology Review, v. 56, p. 1246-1275.

Aydın, F., Karlsi, O., Chen, B., 2008, Petrogenesis of the Neogene alkaline volcanics with imlications for post-collisional lithospheric thinning of the Eastern Pontides, NE Turkey: Lithos, v. 104, p. 249-266.

Aydınçakır, E., and Şen, C., 2013, Petrogenesis of the postcollisional volcanic rocks from the Borçka (Artvin) area: Implications for the evolution of the Eocene magmatism in the Eastern Pontides (NE Turkey): Lithos, v. 172-173, p. 98–117.

Berzina, N., Sotnikov, V.I., Economou-Eliopoulos, M., and Eliopoulos, D.G., 2005, Distribution of rhenium in molybdenite from porphyry Cu-Mo and Mo-Cu deposits of Russia (Siberia) and Mongolia: Ore Geology Reviews, v. 26, p. 91-113.

Bilir, M.E., 2015, Geochemical and geochronological characterization of the Early-Middle Eocene magmatism and related epithermal systems of the Eastern Pontides, Turkey: Unpublished MSc thesis, Muğla, Turkey, Muğla Sıtkı Kocman University, 138 p.

Boztuğ, D., and Harlavan, Y., 2008, K-Ar ages of granitoids unravel the stages of Neo-Tethyan convergence in the Eastern Pontides and central Anatolia, Turkey: International Journal of Earth Sciences, v. 97, p. 585-599.

Boztuğ, D., Erçin, A.I., Kuruçelik, M., Göç, D., Kömür, I., and Iskenderoğlu, A., 2006, Geochemical characteristics of the composite Kaçkar batholith generated in a Neo-Tethyan convergence system, Eastern Pontides, Turkey: Journal of Asian Earth Sciences, v. 27, p. 286-302.

Chen, J.-H., Chung, S.-L., Bingöl, F, A., Lin, C.-Y., and Lin, H.-T., 2016, Zircon U-Pb ages and geochemical constraints on the petrogenesis of Cretaceous to Eocene magmatic rocks in Eastern Pontides, Turkey: In Goldschmidt Conference Proceedings, Yokohama, Japan, June 26th - July 1st 2016, p. 429.

Chen, Y.-J., Wang, P., Li, N., Yang, Y.-F., and Pirajno, F., 2017, The collision-type porphyry Mo deposits in Dabie Shan, China: Ore Geology Reviews, v. 81, p. 405-430.

Çağatay, M.N., 1993, Hydrothermal alteration associated with volcanogenic sulfide deposits: Examples from Turkey: Economic Geology, v. 88, p. 606-621.

Çağatay, M.N. and Boyle, D.R., 1977, Geochemical prospecting for volcanogenic sulfide deposits in the Eastern Black Sea ore province, Turkey: Journal of Geochemical Exploration, v. 8, p. 49-71.

Çınar, S., and Yazıcı, E.N., 1985, Trabzon-Maçka-Güzelyayla köyü bakır-molibden zuhuru ve civarına ait rapor: General Directorate of Mineral Research and Exploration Report (MTA), Report 8025 (in Turkish, unpublished).

Delibaş, O., Moritz, R., Ulianov, A., Chiaradia, M., Saraç, C., Revan, K. M., and Göç, D., 2016, Cretaceous subduction-related magmatism and associated porphyry-type Cu-Mo prospects in the Eastern Pontides, Turkey: New constraints from geochronology and geochemistry: Lithos, v. 248-251, p. 119-137.

Doğan, R., 1980, The granitic rocks and related molybdenite mineralization of the Emeksen area, Espiye, N.E. Turkey: Unpublished thesis, Durham University, Great Britain, 334 p.

Dokuz, A., Karsli, O., Chen, B., and Uysal, İ., 2010, Sources and petrogenesis of Jurassic granitoids in the Yusufeli area, NE Turkey : Implications for pre- and post-collisional lithospheric thinning of the Eastern Pontides: Tectonophysics, v. 480, p. 259-279.

Drábek, M., Rieder, M., and Böhmová, V., 2010, The Re-Mo-S system: new data on phase relations between 400 and 1200°C: European Journal of Mineralogy, v. 22, p. 479-484.

Eğin, D., Hirst, D. M., and Phillips, R., 1979, The petrology and geochemistry of volcanic rocks from the northern Harşit River area, Pontide volcanic province, northeast Turkey: Journal of Volcanology and Geothermal Research, v. 6, p. 105-123.

Er, M., Özdoğan, K., and Tüysüz, N., 1992, Geology and mineralization of Güzelyayla porphyry Cu–Mo occurrence, Trabzon, NE Turkey: In International Symposium on the Geology of the Black Sea region, p. 226-231.

Eyuboglu, Y., 2010, Late Cretaceous high-K volcanism in the Eastern Pontides orogenic belt, and its implications for the geodynamic evolution of NE Turkey: International Geological Review, v. 52, p. 142–186.

Eyuboglu, Y., Santosh, M., Chung, S.L., 2011a, Petrochemistry and U-Pb ages of adakitic intrusions from the Pulur massif (Eastern Pontides, NE Turkey): implications for slab roll-back and ridge subduction associated with Cenozoic convergent tectonics in eastern Mediterranean: Journal of Geology, v. 119, p. 394–417.

Eyuboglu, Y., Santosh, M., and Chung, S.L., 2011b, Crystal fractionation of adakitic magmas in the crust-mantle transition zone: petrology, geochemistry and U-Pb zircon chronology of the Seme adakites, Eastern Pontides, NE Turkey: Lithos, v. 121, p. 151–166.

Eyuboglu, Y., Dudas, F.O., Santosh, M., Yi, K., Kwon, S., and Akaryali, E., 2013, Petrogenesis and U–Pb zircon chronology of adakitic porphyries within the Kop ultramafic massif (Eastern Pontides Orogenic Belt, NE Turkey): Gondwana Research, v. 24, p. 742–766.

Eyuboglu, Y., Santosh, M., Yi, K., Tuysuz, N., Korkmaz, S., Akaryali, E., Dudas, F.O., and Bektas, O., 2014, The Eastern Black Sea-type volcanogenic massive sulfide deposits: Geochemistry, zircon U-Pb geochronology and an overview of the geodynamics of ore genesis: Ore Geology Reviews, v. 59, p. 29-54.

Eyuboglu, Y., Dudas, F.O., Thorkelson, D., Zhu, D.C., Liu, Z., Chatterjee, N., Yi, K., and Santosh, M., 2017, Eocene granitoids of northern Turkey: Polybaric magmatism in an evolving arc-slab window system: Gondwana Research, v. 50, p. 311-345.

Giles, D.L., 1973, Geology and mineralization of the Ulutaş copper–molybdenum deposits, Eastern Anatolia, Turkey: United Nations Development Programme, Technical Report 6, 56p.

Güner, S., and Güç, A.R., 1990, Trabzon-Maçka-Güzelyayla yöresindeki porfiri tip Cu–Mo maden jeolojisi raporu: General Directorate of Mineral Research and Exploration Report (MTA), Report No: 41770 (in Turkish).

JICA, 1987, Report on the cooperative mineral exploration of Gümüşhane area, Follow-up Report: MTA, Ankara, Turkey, unpublished report 8298, 90 p.

Kamitani, M., Takaoğlu, S., Bektaş, O., and Kahaman, İ., 1977, Molybdenum deposits of Çakıldağ Area, Espiye, NE Turkey: General Directorate of Mineral Research and Exploration Report (MTA), v. 6313, 38 p.

Kandemir, R., and Yilmaz, C., 2009, Lithostratigraphy, facies, and deposition environment of the Lower Jurassic Ammonitico Rosso type sediments (ARTS) in the Gümüşhane area, NE Turkey: Implications for the opening of the northern branch of the Neo-Tethys ocean: Journal of Asian Earth Sciences, v. 34, p. 586-598.

Karakaya, M. Ç., Karakaya, N., Küpeli, Ş., and Yavuz, F., 2012, Mineralogy and geochemical behavior of trace elements of hydrothermal alteration types in the volcanogenic massive sulfide deposits, NE Turkey: Ore Geology Reviews, v. 48, p. 197-224.

Karsli, O., Dokuz, A., Faruk, U., and Bin, A., 2010, Relative contributions of crust and mantle to generation of Campanian high-K calc-alkaline I-type granitoids in a subduction setting: Contributions to Mineralogy and Petrology, v. 160, p. 467-487.

Karsli, O., Ketenci, M., Uysal, İ., Dokuz, A., Aydin, F., Chen, B., Kandemir, R., and Wijbrans, J., 2011, Adakite-like granitoid porphyries in the Eastern Pontides, NE Turkey: Potential parental melts and geodynamic implications: Lithos, v. 127, p. 354-372.

Karsli, O., Caran, Ş., Dokuz, A., Çoban, H., Chen, B., and Kandemir, R., 2012, A-type granitoids from the Eastern Pontides , NE Turkey: Records for generation of hybrid A-type rocks in a subduction-related environment: Tectonophysics, v. 531, p. 208-224.

Kaygusuz, A., and Aydınçakır, E., 2011, Petrogenesis of a Late Cretaceous composite pluton from the eastern Pontides: The Dağbaşı pluton, NE Turkey: Neues Jahrbuch für Mineralogie Abhandlungen, v. 188, p. 211–233.

Kaygusuz, A., and Şen, C., 2011, Calc-alkaline I-type plutons in the Eastern Pontides, NE Turkey: U-Pb zircon ages, geochemical and Sr-Nd isotopic compositions: Chemie der Erde, v. 71, p. 59-75.

Kaygusuz, A., and Öztürk,M., 2015, Geochronology, geochemistry, and petrogenesis of the Eocene Bayburt intrusions, Eastern Pontide, NE Turkey: implications for lithospheric mantle and lower crustal sources in the high-K calc-alkaline magmatism: Journal of Asian Earth Sciences, v. 108, p. 97–116.

Kaygusuz, A., Chen, B., Aslan, Z., Wolfgang, S., S¸ Şen, C., 2009, U-Pb zircon SHRIMP ages, geochemical and Sr-Nd isotopic compositions of the Early Cretaceous I type Sarıosman pluton, Eastern Pontides, NE Turkey: Turkish Journal of Earth Sciences, v. 18, p. 549-581.

Kaygusuz, A., Siebel, W., Ilbeyli, N., Arslan, M., Satır, M., and Şen, C., 2010, Insight into magma genesis at convergent plate margins – a case study from the eastern Pontides (NE Turkey): Neues Jahrbuch für Mineralogie - Abhandlungen, v. 187, p. 265–287.

Kaygusuz, A., Sipahi, F., Ilbeyli, N., Arslan, M., Chen, B., and Aydıncakır, E., 2013, Petrogenesis of the Late Cretaceous Turnagöl intrusion in the Eastern Pontides: Implications for magma genesis in the arc setting: Geoscience Frontiers, v. 4, p. 423-438.

Kaygusuz, A., Arslan, M., Siebel, W., Sipahi, F., Nurdane, İ., and Temizel, İ., 2014, LA-ICP MS zircon dating, whole-rock and Sr-Nd-Pb-O isotope geochemistry of the Camiboğazı pluton, Eastern Pontides, NE Turkey: Implications for lithospheric mantle and lower crustal sources in arc-related I-type magmatism: Lithos, v. 195, p. 271-290.

Kazmin, V.G., Sbortshikov, I.M., Ricou, L.-E., Zonenshain, L.P., Boulin, J., and Knipper, A.L., 1986, Volcanic belts as markers of the Mesozoic-Cenozoic active margin of Eurasia: Tectonophysics, v. 123, p. 123-152.

Ketin, İ., 1966, Tectonic units of Anatolia: Bulletin of the MTA Institute, Anakara, Turkey, v. 66, p. 23-33.

Manetti, P., Peccerillo, A., Poli, G., and Corsini, F., 1983, Petrochemical constrains on the models of Cretaceous–Eocene tectonic evolution of the eastern Pontic Chain (Turkey): Cretaceous Research, v. 4, p. 159-172.

Millensifer, T.A., Sinclair, D., Jonasson, I., and Lipmann, A., 2014, Rhenium: In Gunn, G. (ed.), Critical Metals Handbook, John Wiley and Sons, p. 340-360.

Moore, W.J., McKee, E.H., and Akıncı, Ö., 1980, Chemistry and chronology of plutonic rocks in the Pontide mountains, northern Turkey: In Jankovic, S., and Sillitoe, R.H. (eds.), European Copper Deposits, Belgrade University Faculty Geology Mining, Belgrade, p. 209-216.

Moritz, R., Melkonyan, R., Selby, D., Popkhadze, N., Gugushvili, V., Tayan, R., and Ramazanov, V., 2016, Metallogeny of the Lesser Caucasus: From arc construction to postcollision evolution: Society of Economic Geologists Special Publication 19, p. 157-192.

MTA, 1984, Türkiye molibden envanteri, Maden Tetkik Arama Genel Müdürlüğü Yayınları, Ankara 191, 35 p. (in Turkish).

MTA, 2002, 1/500.000 ölçekli Türkiye jeoloji haritası Trabzon paftası: In Akdeniz, N., and Güven, İ. (eds.), General Directorate of Mineral Research and Exploration (MTA) (in Turkish).

Nebioğlu, T.Y., 1983, Trabzon-Maçka-Güxelyayla köyü civarındaki porfiri tip Cu–Mo zuhurlarına ait ön rapor: General Directorate of Mineral Research and Exploration Report (MTA), Report No: 7817 (in Turkish).

Okay, A., 2008, Geology of Turkey: A synopsis: Anschnitt, v. 21, p. 19-42.

Okay, A., and Şahintürk, Ö., 1997, Geology of the Eastern Pontides: In Regional and Petroleum Geology of the Black Sea and Surrounding Region: American Association of Petroleum Geologists Memoir 68, p. 291-311.

Okay, A., and Tüysüz, O., 1999, Tethyan sutures of northern Turkey: Geological Society of London Special Volume 156, p. 475-515.

Okay, A., and Nikishin, A.M., 2015, Tectonic evolution of the southern margin of Laurasia in the Black Sea region: International Geology Review, v. 57, p. 1051-1076.

Okay, A.I., and Topuz, G., 2017, Variscan orogeny in the Black Sea region: International Journal of Earth Sciences, v. 106, p. 569-592.

Peccerillo, A., and Taylor, S.R., 1975, Geochemistry of Upper Cretaceous volcanic rocks from the Pontic chain, Northern Turkey: Bulletin of Volcanology, v. 39, p. 557-569.

Pejatoviç, S., 1979, Metallogeny of the Pontide-type massive sulfide deposits: General Directorate of Mineral Research and Exploration Publication 177, 98 p.

Rathkopf, C., Mazdab, F., Barton, I., and Barton, M.D., 2017, Grain-scale and deposit-scale heterogeneity of Re distribution in molybdenite at the Bagdad porphyry Cu-Mo deposit, Arizona: Journal of Geochemical Exploration, v. 178, p. 45-54.

Revan, M.K., Genç, Y., Maslennikov, V., Maslennikov, V.V., Maslennikov, S.P., Large, R.R. and Danyushevsky, L.V., 2014, Mineralogy and trace-element geochemsitry of sulfide minerals in hydrothermal chimneys from the Upper Cretaceous VMS deposits of the eastern Pontide orogenic belt (NE Turkey): Ore Geology Reviews, v. 63, p. 129-149.

Revan, M.K., Göç D., and Cihan, İ., 2017a, Subduction related ore deposits: In Uysal, I. and Şen, C. (eds.), International Workshop Abstract Book, Post-Conference Field Trip Guide, September 23-26, 2017, Trabzon, p. 36-71.

Revan, M.K., Hisatani, K., Myamoto, H., Delibaş, O., Hanilçi, N., Aysal, N., Özkan, M., Çolak, T., Karsli, Ş., and Peytcheva, I., 2017b, Geology, U-Pb geochronology, and stable isotope geochemistry of the Tunca semi-massive sulfide mineralization, Black sea region, NE Turkey: Implications for ore genesis: Ore Geology Reviews, v. 89, p. 369-389.

Rolland, Y., Sosson, M., Adamia, S., and Sadradze, N., 2011, Prolonged Variscan to Alpine history of an active Eurasian margin (Georgia, Armenia) revealed by $^{40}Ar/^{39}Ar$ dating: Gondwana Research, v. 20, p. 798-815.

Selby, D., and Creaser, R.A., 2001, Late and mid-Cretaceous mineralization in the northern Canadian cordillera: constraints from Re-Os molybdenite dates: Economic Geology, v. 96, p. 1461-1467.

Sillitoe, R.H., 2010, Porphyry copper systems: Economic Geology, v. 105, p. 3-41.

Sinclair, W.D., and Jonasson, I.R., 2014, Highly siderophile elements (Re, Au and PGE) in porphyry deposits and their mantle origins: Acta Geologica Sinica, v. 88, p. 616-618.

Sipahi, F., Kaygusuz,A., Saydam Eker, Ç., Vural, A., and Akpınar, I., 2018, Late Cretaceous arc igneous activity: the Eğrikar monzogranite example: International Geology Review, v. 60, p. 382-400.

Smoliar, M.I., Walker, R.J., and Morgan, J.W., 1996, Re-Os ages of group IIA, IIIA, IVA, and IVB iron meteorites: Science, v. 271, p.1099–1102.

Soylu, M., 1999, Modeling of porphyry copper mineralization of the Eastern Pontides: Unpublished Ph.D. thesis, Ankara, Turkey, Middle East Technical University, 127 p.

Stein, H.J., Markey, R.J., Morgan, J.W., Hannah, J.L., and Scherstén, A., 2001, The remarkable Re-Os chronometer in molybdenite: How and why it works: Terra Nova, v. 13, p. 479-486.

Şen, C., 2007, Jurassic volcanism in the Eastern Pontides: Is it rift related or subduction related? Turkish Journal of Earth Sciences, v. 16, p. 523-539.

Şengör, A.M.C., and Yilmaz, Y., 1981, Tethyan evolution of Turkey: A plate tectonic approach: Tectonophysics, v. 75, p. 181-241.

Şengör, A.M.C., Yilmaz, Y., and Ketin, I., 1980, Remnants of a pre-Late Jurassic ocean in northern Turkey: Fragments of Permian-Triassic paleo-Tethys? Geological Society of America Bulletin, v. 91, p. 599-609.

Taylor, R.P., 1981, Isotope geology of the Bakircay porphyry copper prospect, northern Turkey: Mineralium Deposita, v. 16, p. 375-390.

Taylor, R.P., and Fryer, B.J., 1980, Multiple-stage hydrothermal alteration in porphyry copper system in northern Turkey: the temporal interplay of potassic, propylitic and phyllic fluids: Canadian Journal of Earth Sciences, v. 17, p. 901-927.

Temizel, I., Arslan, M., Ruffet, G., and Peucat, J.J., 2012, Petrochemistry, geochronology and Sr-Nd isotopic systematics of the Tertiary collisional and post-collisional volcanic rocks from the Ulubey (Ordu) area, Eastern Pontide, NE Turkey: Implications for extension-related origin and mantle source characteristics: Lithos, v. 128-131, p. 126-147.

Topuz, G., Altherr, R., Kalt, A., Satir, M., Werner, O., and Schwarz, W.H., 2004a, Aluminous granulites from the Pulur complex, NE Turkey: A case of partial melting, efficient melt extraction and crystallisation: Lithos, v. 72, p. 183-207.

Topuz, G., Altherr, R., and Satir, M., 2004b, Low-grade metamorphic rocks from the Pulur complex, NE Turkey: implications for the pre-Liassic evolution of the Eastern Pontides: International Journal of Earth Sciences, v. 93, p. 72-91.

Topuz, G., Altherr, R., Schwarz, W.H., Siebel, W., Satir, M., and Dokuz, A., 2005, Post-collisional plutonism with adakite-like signatures: The Eocene Saraycik granodiorite (Eastern Pontides, Turkey): Contributions to Mineralogy and Petrology, v. 150, p. 441-455.

Topuz, G., Altherr, R., Schwarz, W.H., Dokuz, A., and Meyer, H.P., 2007, Variscan amphibolite-facies rocks from the Kurtoğlu metamorphic complex (Gümüşhane area, Eastern Pontides, Turkey): International Journal of Earth Sciences, v. 96, p. 861-873.

Topuz, G., Altherr, R., Siebel, W., Schwarz, W.H., Zack, T., Barth, M., Satir, M., and Şen, C., 2010, Carboniferous high-potassium I-type granitoid magmatism in the Eastern Pontides: The Gümüşhane pluton (NE Turkey): Lithos, v. 116, p. 92-110.

Topuz, G., Okay, A., Altherr, R., Schwarz, W.H., Siebel, W., Zack, T., Satir, M., and Şen, C., 2011, Post-collisional adakite-like magmatism in the Agvanis massif and implications for the evolution of the Eocene magmatism in the Eastern Pontides (NE Turkey): Lithos, v. 125, p. 131-150.

Topuz, G., Çelik, Ö.F., Şengör, A.M.C., Altıntaş, E.İ., Zack, T., Rolland, Y., and Barth, M., 2013, Jurassic ophiolite formation and emplacement as backstop to a subduction-accretion complex in Northeast Turkey, the Refahiye ophiolite, and relation to the Balkan ophiolites: American Journal of Science, v. 313, p. 1054-1087.

Ustaömer, T., and Robertson, A.H.F., 2010, Late Palaeozoic-Early Cenozoic tectonic development of the Eastern Pontides (Artvin area), Turkey: stages of closure of Tethys along the southern margin of Eurasia: Geological Society of London Special Publication 340, p. 281-327.

Ustaömer, T., Robertson, A.H.F., Ustaömer, P.A., Gerdes, A., and Peytcheva, I., 2012, Constraints on Variscan and Cimmerian magmatism and metamorphism in the Pontides (Yusufeli-Artvin area), NE Turkey from U-Pb dating and granite geochemistry: Geological Society of London Special Publication 372, v. 49-74.

Voudouris, P., and Melfos, V., 2012, Aluminum-phosphate-sulfate (APS) minerals in the sericitic-advanced argillic alteration zone of the Melitena porphyry- epithermal Mo-Cu±Au±Re prospect, western Thrace, Greece: Neues Jahrbuch für Mineralogie Abhandlungen, v. 190-191, p. 11-27.

Voudouris, P. C., Melfos, V., Spry, P. G., Bindi, L., Kartal, T., Arikas, K., Moritz, R., and Ortelli, M., 2009, Rhenium-rich molybdenite and rheniite in the Pagoni Rachi Mo-Cu-Te-Ag-Au prospect, northern Greece: Implications for the Re geochemistry of porphyry-style Cu-Mo and Mo mineralization: The Canadian Mineralogist, v. 47, p. 1013–1168.

Voudouris, P., Melfos, V., Spry, P.G., Bindi, L., Moritz, R., Ortelli, M., and Kartal, T., 2013, Extremely Re-rich molybdenite from porphyry Cu-Mo-Au prospects in northeastern Greece: Mode of occurrence, causes of enrichment, and implications for gold exploration: Minerals, v. 3, p. 165-191.

Yigit, O., 2009, Mineral deposits of Turkey in relation to Tethyan metallogeny: Implications for future mineral exploration: Economic Geology, v. 104, p.19-51.

Yilmaz, S., and Boztuğ, D., 1996, Space and time relations of three plutonic phases in the Eastern Pontides, Turkey: International Geology Reviews, v. 38, p. 935-956.

Yilmaz, Y., and Tüysüz, O., 1997, Geology and tectonic evolution of the Pontides: In Regional and petroleum geology of the Black Sea and surrounding Region: American Association of Petroleum Geologists Memoir 68, p. 183-226.

Yilmaz, A., Adamia, S., Chabukiani, A., Chkhotua, T., Erdogan, K., Tuzcu, S., and Karabiyiko Glu, M., 2000, Structural correlation of the Southern Transcaucasus (Georgia)-Eastern Pontides (Turkey): Geological Society of London Special Publication 173, p. 171-182.

Yilmaz, S., Güngör, Y., and Boztuğ, D., 2004, Comparative petrogenetic investigation of composite Kaçkar batholith granitoids in Eastern Pontide magmatic arc - Northern Turkey: Earth, Planets and Space, v. 56, p. 429-446.

Yılmaz-Şahin, S., 2005, Transition from arc- to post-collision extensional setting revealed by K-Ar dating and petrology: An example from the granitoids of the eastern Pontide igneous Terrane, Araklı-Trabzon, NE Turkey: Geological Journal, v. 40, p. 425–440.

Zhong, J., Chen, Y.-J., and Pirajno, F., 2016, Geology, geochemistry and tectonic settings of the molybdenum deposits in South China: A review: Ore Geology Reviews, v. 81, p. 829-855.

Figure Captions

Figure 1: Simplified regional geological map with location of the major ore deposits of the Eastern Pontides, and the Elbeyli, Emeksen, Güzelyayla and Ispir-Ulutaş porphyry systems investigated in this contribution (modified after MTA, 2002, and Delibaş et al., 2016). Inset shows major tectonic units of Anatolia (simplified after Ketin, 1966).

Figure 2: Simplified geological map of the Elbeyli prospect with the outline of the mapped alteration zones and the main quartz-molybdenite vein area. The U-Pb zircon age of the Late Cretaceous monzonite/monzodiorite is from Delibaş et al. (2016).

Figure 3: Mineralization styles and alteration minerals at the Elbeyli prospect. (a) Quartz-pyrite-chalcopyrite stockwork hosted by Late Cretaceous andesite. (b) NW-oriented quartz-pyrite-enargite-chalcopyrite-tennantite-molybdenite vein in Late Cretaceous andesite. (c) NW-oriented quartz-molybdenite vein hosted by monzonite/monzodiorite. (d) Silicified zone enriched in molybdenite in Late Cretaceous andesite. (e) Alteration minerals along NW-striking quartz-molybdenite veins, including zunyite, pyrophyllite and quartz, polarized transmitted light. (f) Zunyite associated with quartz in the advanced argillic alteration zone. (g) Enargite and euhedral pyrite replaced by tennantite along rims and fractures, polarized reflected light. (h) Molybdenite filling fractures of vein and disseminated pyrite, polarized reflected light. Abbreviations: eng-enargite, mol-molybdenite, prl-pyrophyllite, py-pyrite, qz-quartz, tnt-tennantite, zun-zunyite.

Figure 4: Simplified geological map of the Emeksen prospect after Kamitani et al. (1977), and location of the main quartz-molybdenite vein zones from Doğan, (1980). The U-Pb zircon ages of the Late Cretaceous intrusions are from Delibaş et al. (2016).

Figure 5: Mineralization and alteration styles at the Emeksen prospect. (a) North-oriented quartz-pyrite-molybdenite vein hosted by granite affected by sericitic alteration. (b) Quartz-molybdenite-pyrite stockwork hosted by granite. (c) Disseminated molybdenite in silicified porphyritic granite. (d) Quartz-pyrite-molybdenite banded vein in silicified porphyritic granite. (e) Native gold, electrum and arsenopyrite in quartz. (f) Secondary biotite vein crosscuting granodiorite, with chlorite replacement of biotite, plain transmitted light. Abbreviations: amp-amphibole, apy-arsenopyrite, Au-native gold, bt-biotite, chl-chlorite, el-electrum, kfs-K feldspar, mol-molybdenite, py-pyrite, qz-quartz.

Figure 6: Simplified geological map of the Güzelyayla deposit after Güner and Güç (1990), with the outline of the mapped alteration zones and the main disseminated and vein molybdenite area modified after JICA (1987). The U-Pb zircon age of the Late Cretaceous porphyritic dacite is from Delibaş et al. (2016), and the $^{40}Ar/^{39}Ar$ ages of the Eocene granodioritic to tonalitic porphyryitic dikes are from Karsli et al. (2011).

Figure 7: Mineralization and alteration styles at the Güzelyayla deposit. (a) Quartz-pyrite-chalcopyrite stockwork hosted by Late Cretaceous andesite. (b) Quartz-molybdenite stockwork hosted by porphyritic dacite containing disseminated chalcopyrite and pyrite. (c) Late stage quartz-pyrite-molybdenite vein crosscutting Late Cretaceous andesite with disseminated pyrite and chalcopyrite. (d) Thin quartz and sericite veins crosscutting the potassic alteration zone in porphyritic dacite. (e) Pyrite-molybdenite-chalcopyrite assemblage of the stockwork veins, plain

reflected light (pyrrhotite and rutile are not shown). (f) Supergene covellite, chalcocite and digenite affecting the primary chalcopyrite-pyrite assemblage. Abbreviations: cct-chalcocite, ccp: chalcopyrite, cv-covellite, dg-digenite, mol-molybdenite, py-pyrite, qz-quartz.

Figure 8: Simplified geological map of the Ispir-Ulutaş deposit (simplified after Giles, 1973) with the outline of the mapped alteration zones and the main disseminated and vein molybdenite area modified after Revan et al. (2017a). The outline of the skarn area is from http://www.demirexport.com (see Revan et al., 2017a, page 57). The U-Pb zircon age of the Late Cretaceous intrusions are from Delibaş et al. (2016).

Figure 9: Mineralization and alteration styles at the Ispir-Ulutaş deposit. (a) Quartz-pyrite-chalcopyrite-molybdenite stockwork hosted by quartz porphyry. (b) Late stage NW-oriented quartz-pyrite-molybdenite vein crosscutting a quartz-pyrite-chalcopyrite-molybdenite stockwork hosted by quartz porphyry. (c) Pyrite-chalcopyrite-sphalerite-hematite assemblage within the stockwork vein system (molybdenite not shown). (d) Pervasive sericitic alteration assemblage including sericite, muscovite and quartz. Abbreviations: ccp-chalcopyrite, hem-hematite, mol-molybdenite, ms-muscovite, py-pyrite, qz-quartz, ser-sericite, sl-sphalerite.

Figure 10: Molybdenum vs. rhenium contents obtained by EMPA for molybdenite samples from the Elbeyli prospect and the Güzelyayla deposit (Table 2), and Re contents obtained by mass spectrometry for molybdenite samples from the Elbeyli, Emeksen, Güzelyayla and Ispir-Ulutaş study areas (Table 1). Rhenium concentrations of molybdenite sampled at the Emeksen prospect and the Ispir-Ulutaş deposit remained below the EMPA detection limit of 0.8 wt%.

Figure 11: (a) Published U-Pb and $^{40}Ar/^{39}Ar$ ages of magmatic rocks from the Turkish Eastern Pontides, together with the molybdenite Re-Os dates obtained in this study for the Elbeyli, and the Emeksen prospects, and the Güzelyayla and Ispir-Ulutaş deposits (red box symbols). (b) Ages of ore forming events in the Lesser Caucasus, Paleogene ore-forming events and volcanic host rocks of VMS deposits in the Eastern Pontides. References: 1 - Boztuğ and Harlavan (2008); 2 – Giles (2003); 3 - Delibaş et al. (2016); 4 – Chen et al. (2016); 5 – Moore et al. (1980); 6 - Aydın (2014); 7 – Eyuboglu (2010); 8 – Karsli et al. (2010); 9 - Yilmaz-Şahin (2005); 10 - Kaygusuz and Aydınçakır (2011); 11 – Kaygusuz et al. (2009); 12 – Karsli et al. (2012); 13 - Kaygusuz et al. (2010); 14 - Kaygusuz and Şen (2011); 15 – Sipahi et al. (2018); 16 - Kaygusuz et al. (2013); 17 - Kaygusuz et al. (2014); 18 – Eyuboglu et al. (2013); 19 - Eyuboglu et al. (2011a); 20 - Eyuboglu et al. (2011b); 21 – Topuz et al. (2011); 22 - Kaygusuz and Öztürk (2015); 23 - Karsli et al. (2011); 24 - Aydınçakır and Şen (2013); 25 - Eyuboglu et al. (2017); 26 – Moritz et al. (2016); 27 - Eyuboglu et al. (2014); 28 – Revan et al. (2017b); 29 – Soylu (1999); 30 – Yigit (2009); 31 – Bilir (2015); 32 – Taylor (1981).

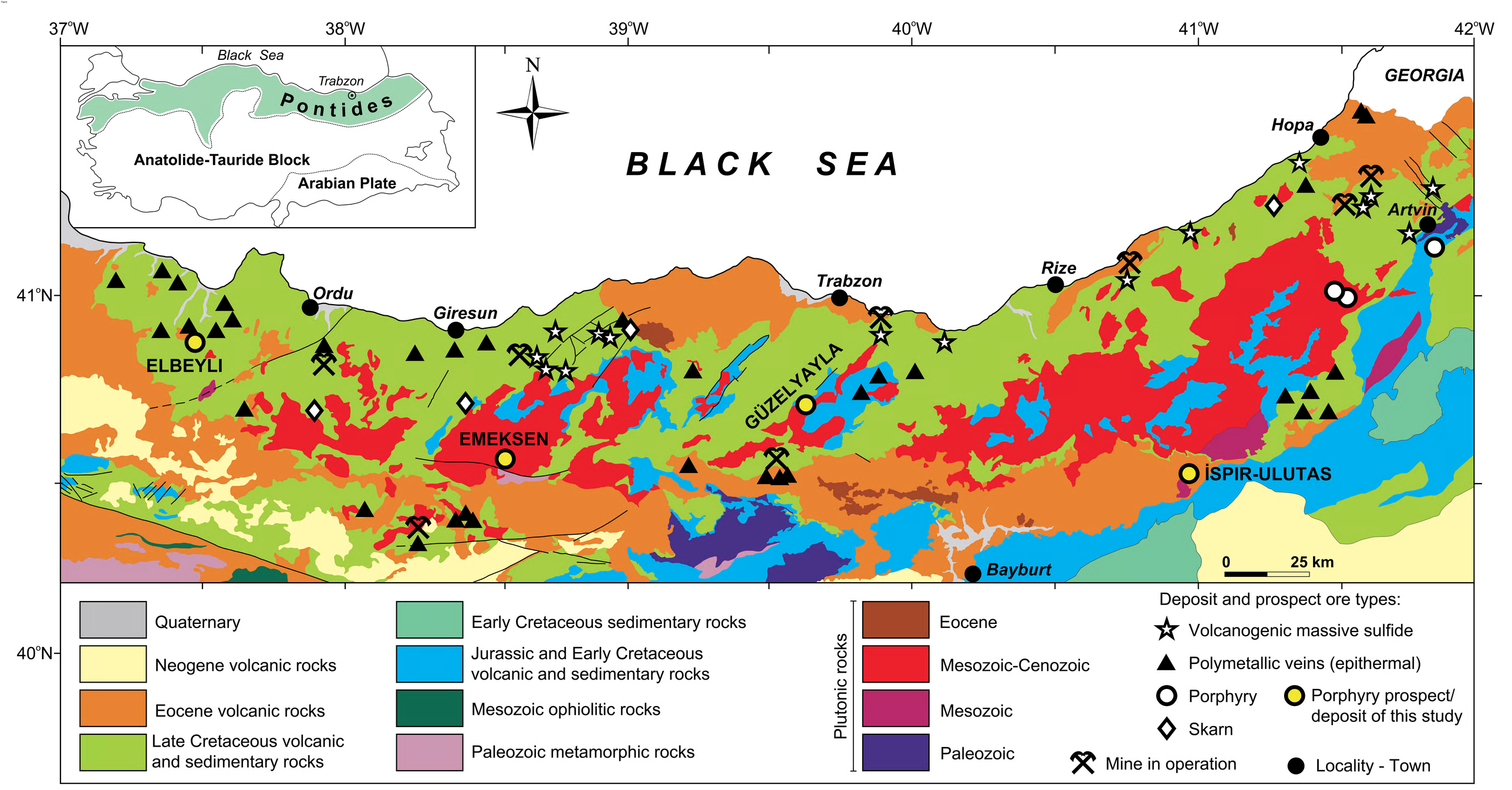
37°W
38°W
39°W
40°W
41°W
42°W
41°N
40°N
Black Sea
Trabzon
Pontides
Anatolide-Tauride Block
Arabian Plate
N
BLACK SEA
GEORGIA
Hopa
Artvin
Rize
Trabzon
Ordu
Giresun
ELBEYLI
EMEKSEN
GÜZELYAYLA
İSPIR-ULUTAS
Bayburt
0
25 km
Quaternary
Neogene volcanic rocks
Eocene volcanic rocks
Late Cretaceous volcanic and sedimentary rocks
Early Cretaceous sedimentary rocks
Jurassic and Early Cretaceous volcanic and sedimentary rocks
Mesozoic ophiolitic rocks
Paleozoic metamorphic rocks
Plutonic rocks
Eocene
Mesozoic-Cenozoic
Mesozoic
Paleozoic
Deposit and prospect ore types:
Volcanogenic massive sulfide
Polymetallic veins (epithermal)
Porphyry
Porphyry prospect/ deposit of this study
Skarn
Mine in operation
Locality - Town

Fig. 1

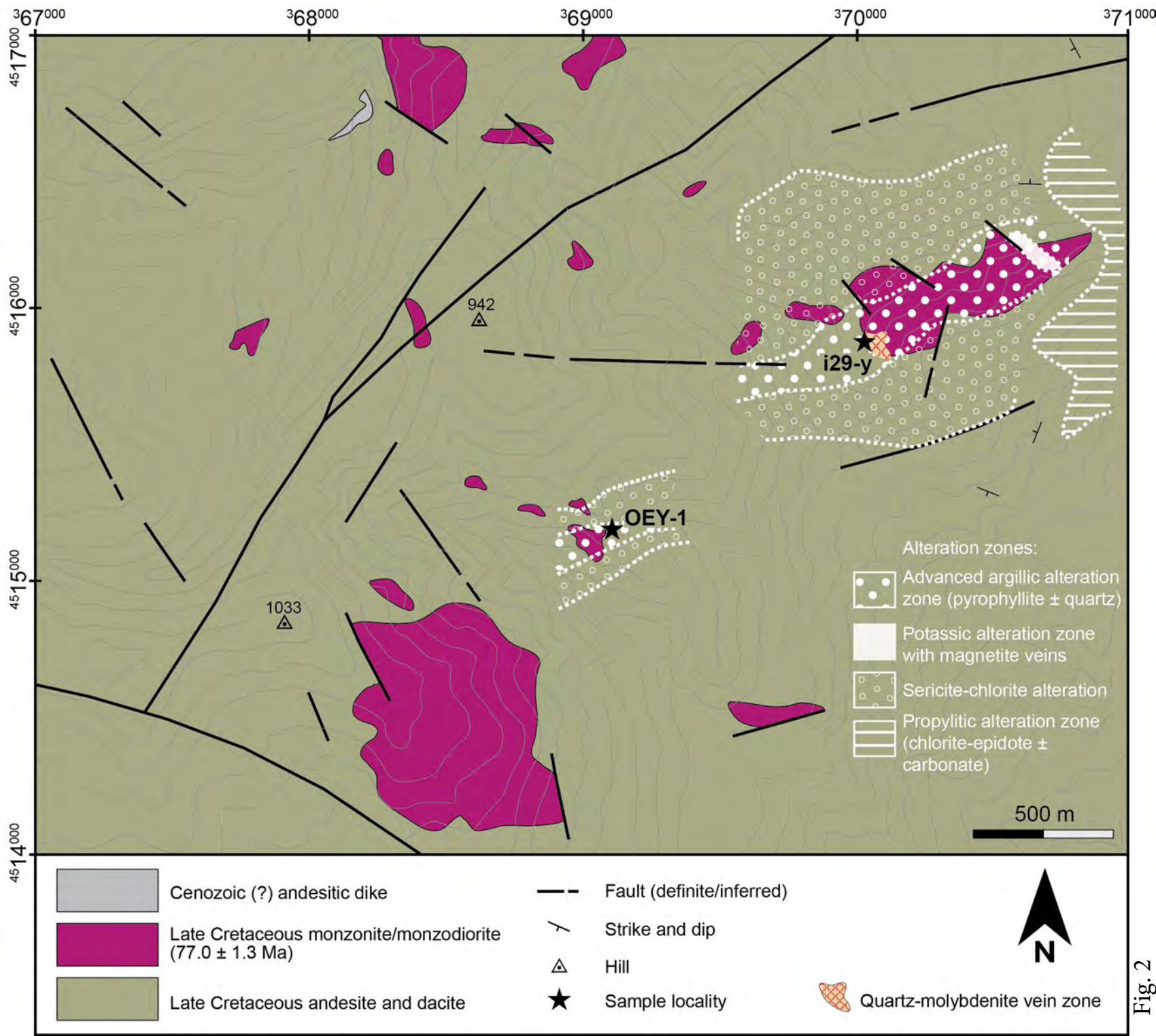
367000
368000
369000
370000
371000
4517000
4516000
4515000
4514000
942
1033
i29-y
OEY-1
Alteration zones:
Advanced argillic alteration zone (pyrophyllite ± quartz)
Potassic alteration zone with magnetite veins
Sericite-chlorite alteration
Propylitic alteration zone (chlorite-epidote ± carbonate)
500 m
Cenozoic (?) andesitic dike
Late Cretaceous monzonite/monzodiorite (77.0 ± 1.3 Ma)
Late Cretaceous andesite and dacite
Fault (definite/inferred)
Strike and dip
Hill
Sample locality
Quartz-molybdenite vein zone
N

Fig. 2

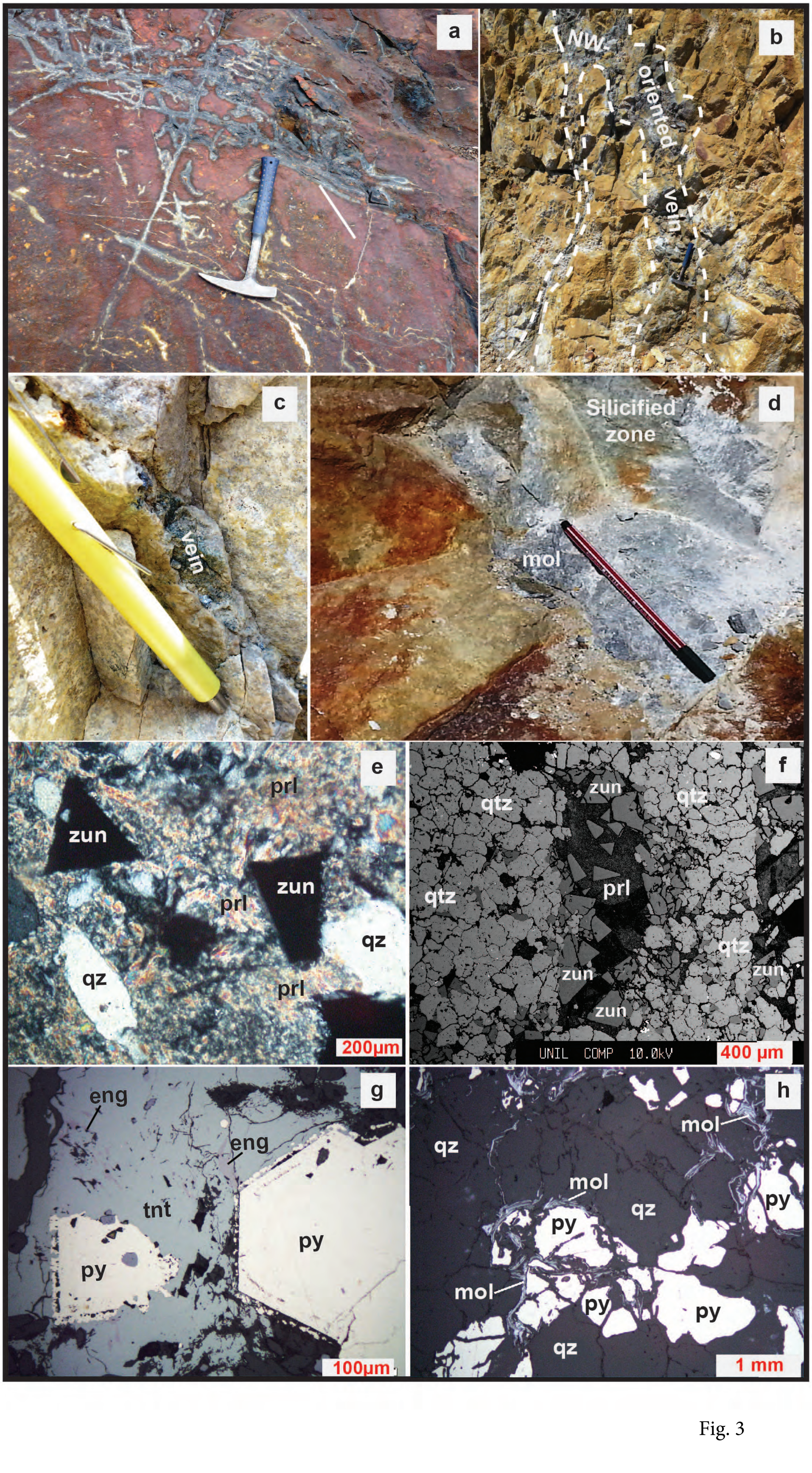
a
b
NW-oriented vein
c
vein
d
Silicified zone
mol
e
prl
zun
zun
prl
qz
qz
prl
200µm
f
zun
qtz
qtz
qtz
prl
qtz
zun
zun
zun
UNIL COMP 10.0kV
400 µm
g
eng
eng
tnt
py
py
100µm
h
mol
qz
mol
py
qz
py
mol
py
py
qz
1 mm

Fig. 3

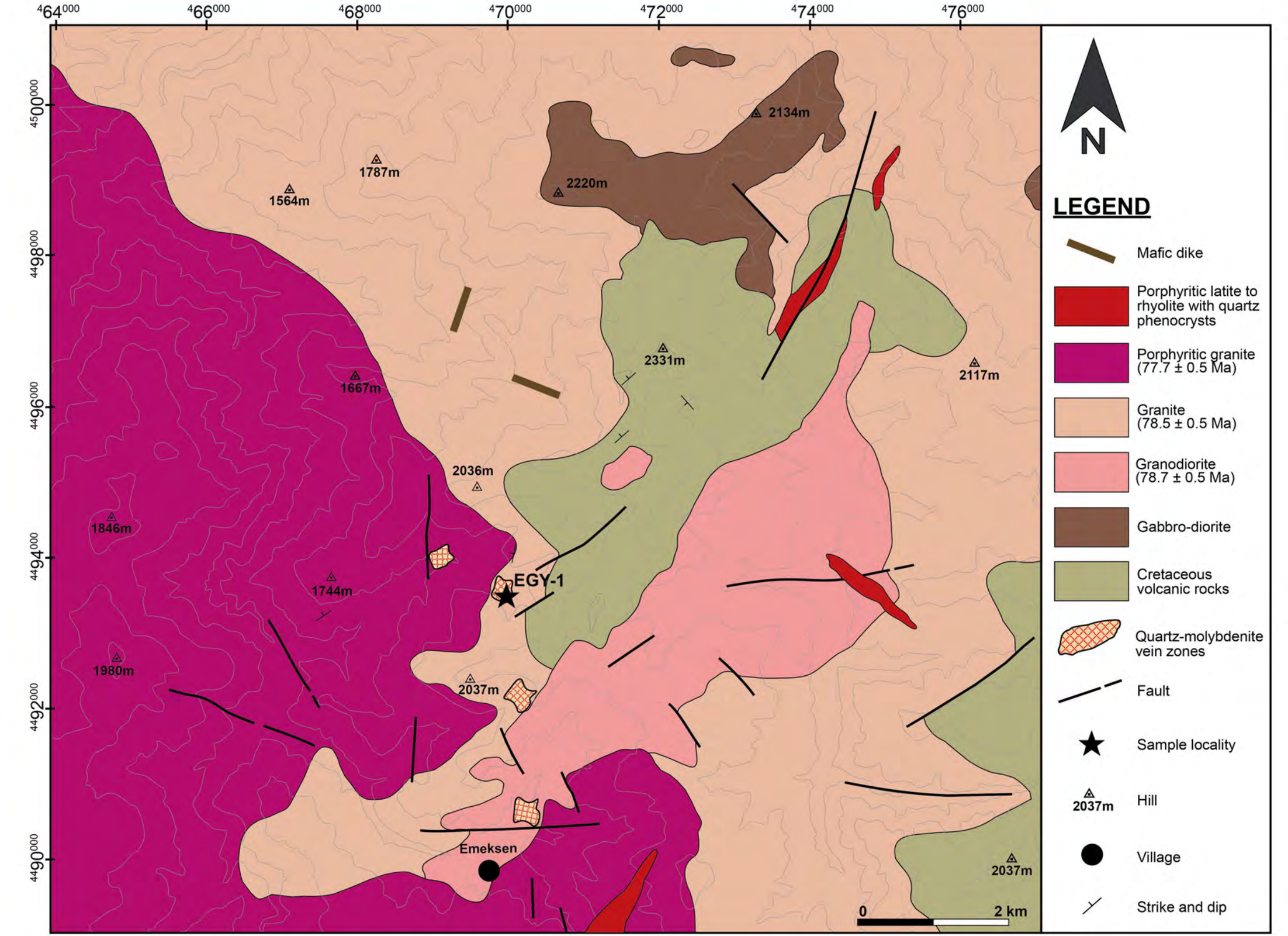
464000
466000
468000
470000
472000
474000
476000
4500000
4498000
4496000
4494000
4492000
4490000
N
2134m
1787m
2220m
1564m
2331m
2117m
1667m
2036m
1846m
1744m
EGY-1
1980m
2037m
Emeksen
2037m
0
2 km
LEGEND
Mafic dike
Porphyritic latite to rhyolite with quartz phenocrysts
Porphyritic granite (77.7 ± 0.5 Ma)
Granite (78.5 ± 0.5 Ma)
Granodiorite (78.7 ± 0.5 Ma)
Gabbro-diorite
Cretaceous volcanic rocks
Quartz-molybdenite vein zones
Fault
Sample locality
2037m
Hill
Village
Strike and dip

Fig. 4

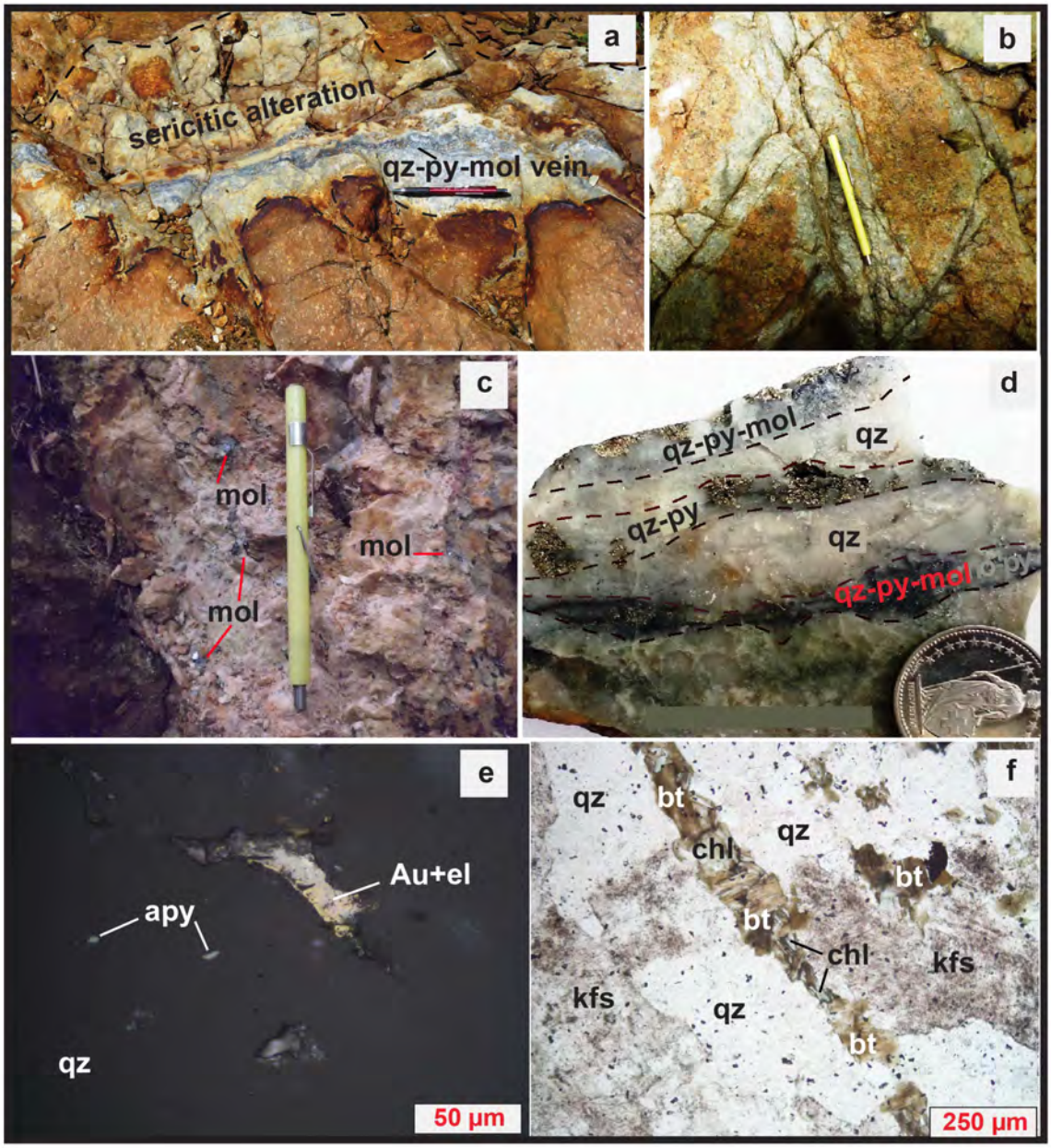
a
sericitic alteration
qz-py-mol vein
b
c
mol
mol
mol
d
qz-py-mol
qz
qz-py
qz
qz-py-mol
e
Au+el
apy
qz
50 µm
f
qz
bt
qz
chl
bt
bt
chl
kfs
kfs
qz
bt
250 µm

Fig. 5

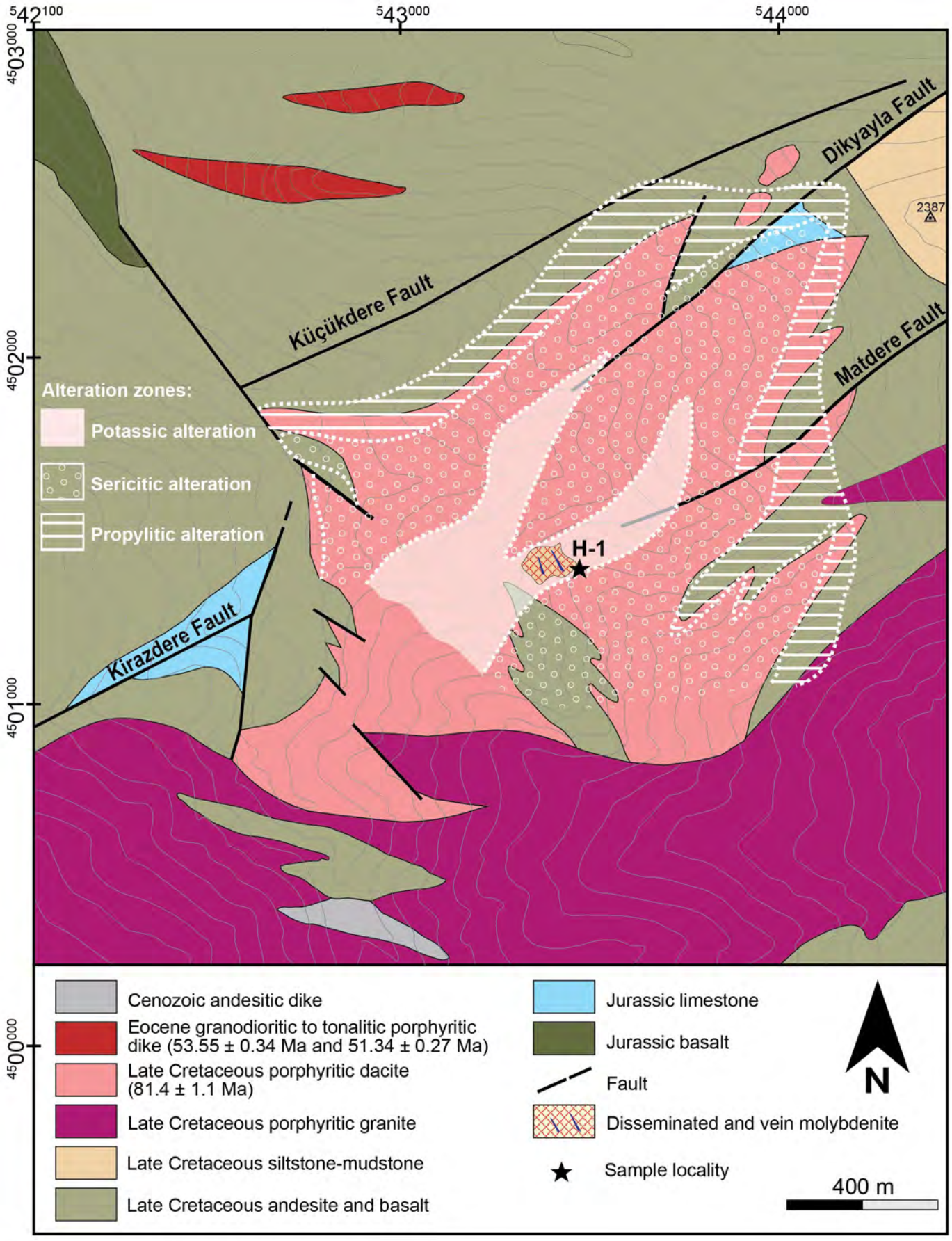
5 42 100
5 43 000
5 44 000
4503000
4502000
4501000
4500000
Dikyayla Fault
Küçükdere Fault
Matdere Fault
Kirazdere Fault
2387
H-1
Alteration zones:
Potassic alteration
Sericitic alteration
Propylitic alteration
Cenozoic andesitic dike
Eocene granodioritic to tonalitic porphyritic dike (53.55 ± 0.34 Ma and 51.34 ± 0.27 Ma)
Late Cretaceous porphyritic dacite (81.4 ± 1.1 Ma)
Late Cretaceous porphyritic granite
Late Cretaceous siltstone-mudstone
Late Cretaceous andesite and basalt
Jurassic limestone
Jurassic basalt
Fault
Disseminated and vein molybdenite
Sample locality
N
400 m

Fig. 6

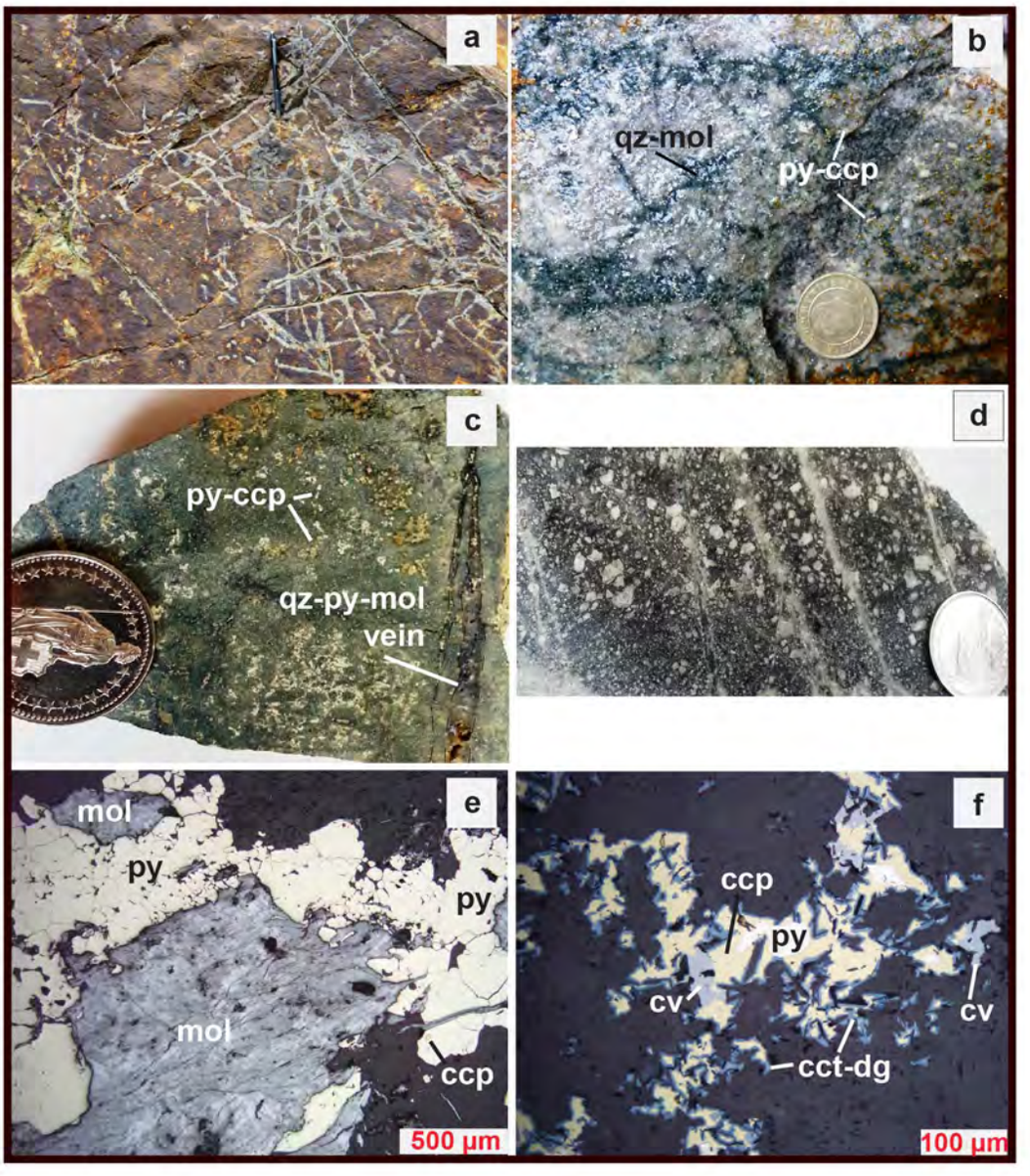
a
b
qz-mol
py-ccp
c
py-ccp
qz-py-mol
vein
d
e
mol
py
py
mol
ccp
500 µm
f
ccp
py
cv
cv
cct-dg
100 µm

Fig. 7

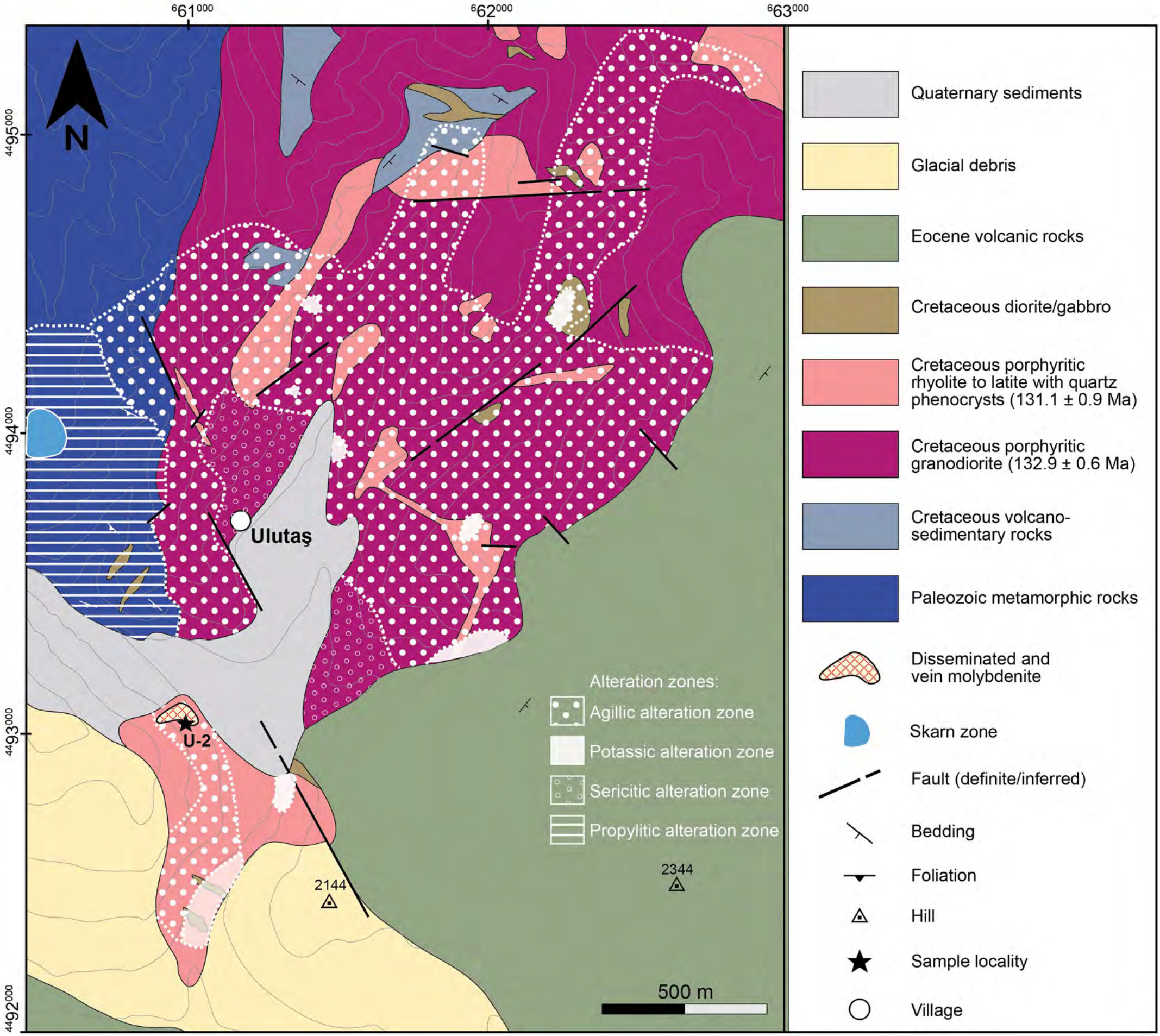
6 61 000
6 62 000
6 63 000
44 95 000
44 94 000
44 93 000
44 92 000
N
Ulutaş
U-2
2144
2344
Alteration zones:
Agillic alteration zone
Potassic alteration zone
Sericitic alteration zone
Propylitic alteration zone
500 m
Quaternary sediments
Glacial debris
Eocene volcanic rocks
Cretaceous diorite/gabbro
Cretaceous porphyritic rhyolite to latite with quartz phenocrysts (131.1 ± 0.9 Ma)
Cretaceous porphyritic granodiorite (132.9 ± 0.6 Ma)
Cretaceous volcano-sedimentary rocks
Paleozoic metamorphic rocks
Disseminated and vein molybdenite
Skarn zone
Fault (definite/inferred)
Bedding
Foliation
Hill
Sample locality
Village

Fig. 8

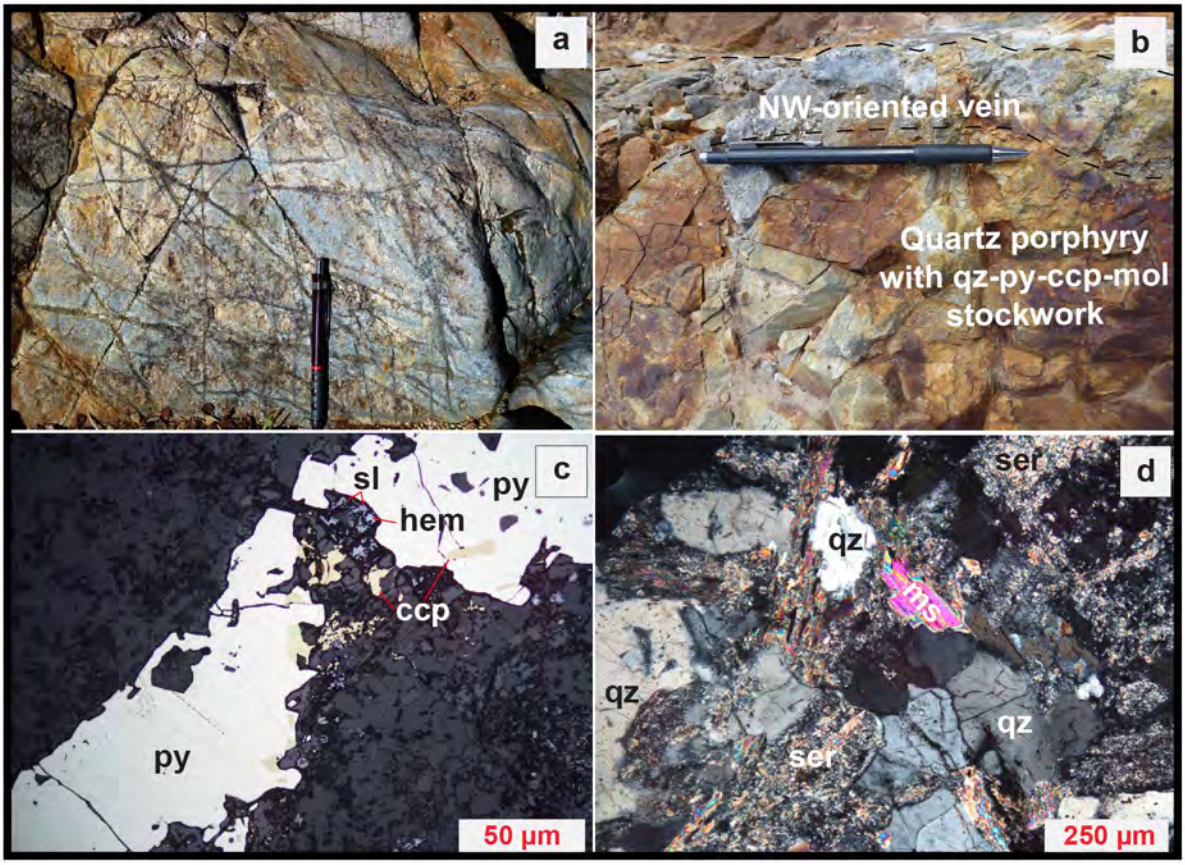
a
b
NW-oriented vein
Quartz porphyry
with qz-py-ccp-mol
stockwork
c
sl
py
hem
ccp
py
50 µm
d
ser
qz
ms
qz
qz
ser
250 µm

Fig. 9

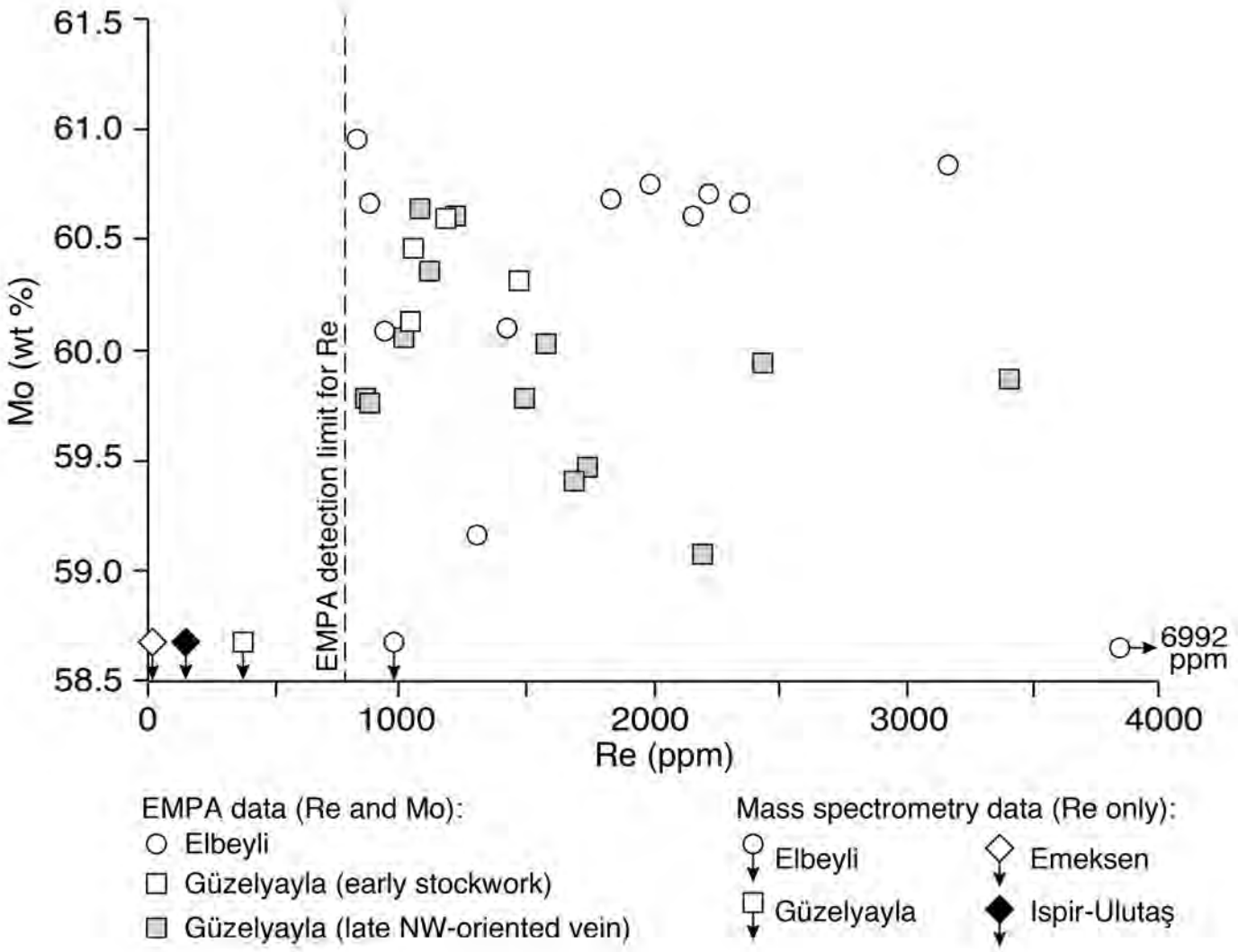
61.5
61.0
60.5
60.0
59.5
59.0
58.5
Mo (wt %)
EMPA detection limit for Re
6992 ppm
0
1000
2000
3000
4000
Re (ppm)
EMPA data (Re and Mo):
Elbeyli
Güzelyayla (early stockwork)
Güzelyayla (late NW-oriented vein)
Mass spectrometry data (Re only):
Elbeyli
Emeksen
Güzelyayla
Ispir-Ulutaş

Fig. 10

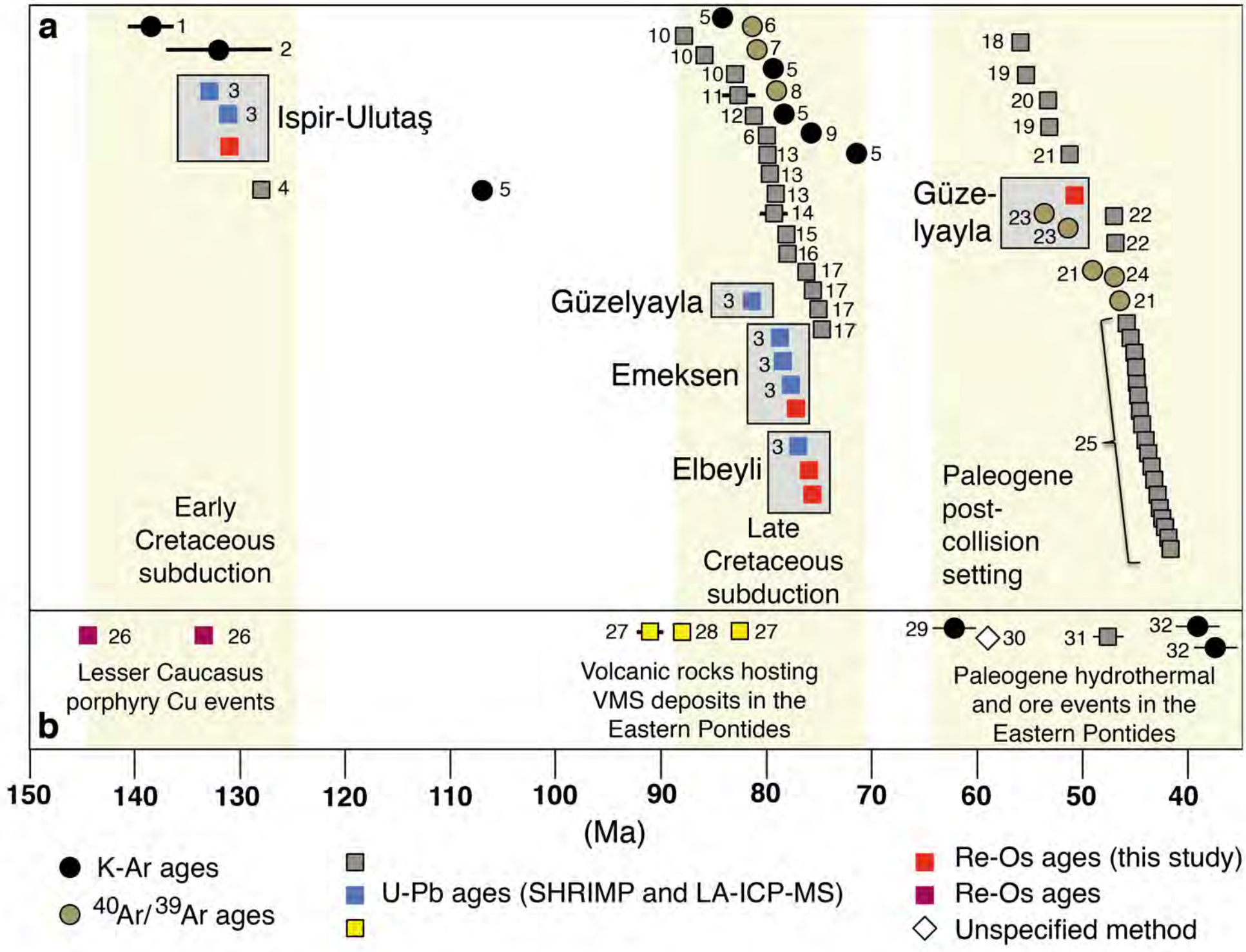
a
Ispir-Ulutaş
Early Cretaceous subduction
Güzelyayla
Emeksen
Elbeyli
Late Cretaceous subduction
Güze-lyayla
Paleogene post-collision setting
Lesser Caucasus porphyry Cu events
Volcanic rocks hosting VMS deposits in the Eastern Pontides
Paleogene hydrothermal and ore events in the Eastern Pontides
b
150
140
130
120
110
100
90
80
70
60
50
40
(Ma)
K-Ar ages
40Ar/39Ar ages
U-Pb ages (SHRIMP and LA-ICP-MS)
Re-Os ages (this study)
Re-Os ages
Unspecified method

Fig. 11

Table 1 - Re-Os data of molybdenite from the Elbeyli, Emeksen, Ispir-Ulutaş and Güzelyayla study areas in the Eastern Pontides

Sample	Study area	wt (g)	Re (ppm) ±2σ	^{187}Re (ppm) ±2σ	^{187}Os (ppb) ±2σ	Age (Ma) ± 2σ (1)	Age (Ma) ± 2σ (2)
OEY-1	Elbeyli	0.0052	6991.7±58.0	4394.4±36.5	5571.5±45.0	76.0±0.3	76.0±0,4
i29Y	Elbeyli	0.0107	979.9±4.8	615.9±3.0	776.7±3.5	75.7±0.3	75.7±0.4
EGY-1	Emeksen	0.0044	9.7±0.1	6.1±0.08	7.9±0.1	77.2±0.9	77.2±1
U-2	Ispir-Ulutaş	0.0106	150.3±0.7	94.4±0.5	206.3±0.9	130.1±0.5	130.1±0,7
H-1	Güzelyayla	0.0108	367.7±1.8	231.1±1.1	195.3±0.9	50.7±0.2	50.7±0.3

Re-Os dates are calculated using Re decay constants from Smoliar et al. (1996).

(1) Age uncertainty includes all sources of analytical uncertainty.

(2) Age uncertainty includes all sources of analytical uncertainty and that of the decay constant.

Table 2 - Composition of molybdenite samples obtained by EMPA, including S, Mo and Re concentrations

Sample-spot	Study area	S (wt%)	Mo (wt%)	Re (wt%)	Total (wt%)	Sample-spot	Study area	S (wt%)	Mo (wt%)	Re (wt%)	Total (wt%)
H1-2	Güzelyayla*	38.85	60.63	b.d.	99.49	I29-1	Elbeyli	40.42	60.48	b.d.	100.90
H1-3	Güzelyayla*	39.34	60.34	b.d.	99.68	I29-4	Elbeyli	40.13	60.70	0.2223	101.06
H1-6	Güzelyayla*	40.87	60.04	b.d.	100.91	I29-5	Elbeyli	38.09	60.67	0.2349	98.99
H1-7	Güzelyayla*	40.98	60.60	0.1174	101.70	I29-6	Elbeyli	38.93	60.84	0.3162	100.09
H1-9	Güzelyayla*	39.59	60.67	b.d.	100.26	I29-7	Elbeyli	39.52	60.42	b.d.	99.95
H1-11	Güzelyayla*	39.73	60.37	b.d.	100.11	I29-8	Elbeyli	39.81	60.08	0.0939	99.98
H1-12	Güzelyayla*	38.95	60.44	b.d.	99.40	I29-9	Elbeyli	40.41	60.75	0.1988	101.35
H1-13	Güzelyayla*	39.84	60.42	b.d.	100.26	I29-11	Elbeyli	40.69	60.10	0.1427	100.93
H1-14	Güzelyayla*	40.59	60.12	0.103	100.80	I29-12	Elbeyli	40.16	60.29	b.d.	100.44
H1-15	Güzelyayla*	40.17	60.22	b.d.	100.40	I29-13	Elbeyli	38.82	60.96	0.082	99.85
H1-16	Güzelyayla*	39.59	60.33	b.d.	99.92	I29-15	Elbeyli	40.15	60.07	b.d.	100.23
H1-17	Güzelyayla*	40.00	60.48	b.d.	100.48	I29-21	Elbeyli	40.17	60.34	b.d.	100.52
H1-18	Güzelyayla*	39.64	60.30	0.1469	100.09	I29-23	Elbeyli	37.79	59.16	0.1295	97.08
H1-20	Güzelyayla*	41.28	60.45	0.1049	101.84	I29-25	Elbeyli	40.14	60.66	0.0867	100.89
TMM1-1	Güzelyayla**	40.80	59.77	0.0849	100.66	I29-26	Elbeyli	39.89	60.85	b.d.	100.74
TMM1-2	Güzelyayla**	40.78	60.03	0.1576	100.97	I29-27	Elbeyli	39.96	61.04	b.d.	101.00
TMM1-3	Güzelyayla**	40.31	59.07	0.2198	99.60	I29-28	Elbeyli	40.84	60.61	0.2157	101.67
TMM1-4	Güzelyayla**	40.09	59.46	0.1741	99.73	I29-30	Elbeyli	40.21	60.68	0.1831	101.07
TMM1-5	Güzelyayla**	40.58	59.40	0.1693	100.15	GEM6-5	Emeksen	40.38	60.60	b.d.	100.98
TMM1-6	Güzelyayla**	40.02	59.84	b.d.	99.86	GEM6-6	Emeksen	40.32	60.56	b.d.	100.89
TMM1-7	Güzelyayla**	40.48	60.05	0.1019	100.63	GEM6-17	Emeksen	39.56	60.62	b.d.	100.18
TMM1-8	Güzelyayla**	40.08	60.64	0.1076	100.83	GEM6-18	Emeksen	40.23	60.35	b.d.	100.59
TMM1-9	Güzelyayla**	40.01	59.94	0.2431	100.19	GEM6-20	Emeksen	40.32	61.05	b.d.	101.38
TMM1-10	Güzelyayla**	40.11	60.36	0.111	100.58	GEM6-21	Emeksen	39.68	60.03	b.d.	99.71
TMM1-11	Güzelyayla**	38.93	59.86	0.3409	99.13	GEM6-22	Emeksen	39.43	59.86	b.d.	99.29
TMM1-12	Güzelyayla**	40.11	59.78	0.1493	100.03	GEM6-23	Emeksen	39.96	60.17	b.d.	100.13
TMM1-14	Güzelyayla**	40.15	60.60	0.1216	100.88	GEM6-24	Emeksen	38.82	60.13	b.d.	98.95
TMM1-15	Güzelyayla**	39.50	59.76	0.0873	99.34	GEM6-25	Emeksen	40.38	60.47	b.d.	100.85
U2-2	Ispir-Ulutas	39.96	59.89	b.d.	99.85	GEM6-26	Emeksen	40.40	60.52	b.d.	100.91
U2-3	Ispir-Ulutas	40.68	60.58	b.d.	101.26	GEM6-28	Emeksen	40.07	60.40	b.d.	100.47
U2-4	Ispir-Ulutas	40.51	60.80	b.d.	101.30						

Güzelyayla*: molybdenite from early stockwork veins (Fig. 7a-b).

Güzelyayla**: molybdenite from late stage NW-oriented veins (Fig. 7c).

b.d.: below EMPA detection limit.